CoDCon Project: Final Report

Nuclear Technology Research and Development

Prepared for
U.S. Department of Energy
Materials Recovery and Waste Form Development

GJ Lumetta, JR Allred, SE Asmussen, SA Bryan, JC Carter, GB Hall, FD Heller, AM Lines, and SI Sinkov
Pacific Northwest National Laboratory
C Pereira
Argonne National Laboratory

October 2020

PNNL-30604

SUMMARY

The co-decontamination (CoDCon) project was established in FY 2016 with the objectives of (a) evaluating the uncertainty in the uranium (U)/plutonium (Pu) ratio in a mixed U/Pu product from a tributyl phosphate (TBP)–based solvent extraction flowsheet, and (b) developing and demonstrating on-line optical spectroscopy for real-time monitoring of key components (e.g., Pu, U, and HNO_3 concentrations) in the process solutions. We were interested in assessing the accuracy and precision to which a specific uranium-to-plutonium (U/Pu) ratio can be achieved, which for the purposes of this project was set at a U/Pu mass ratio of 7/3. The uncertainty associated with achieving this specific target U/Pu ratio was investigated during five flowsheet tests using laboratory-scale solvent extraction equipment. In addition, optical spectroscopic techniques were incorporated into the CoDCon solvent extraction testing system, allowing real time monitoring of all input and output process streams.

Two CoDCon flowsheet tests were performed in FY 2018 using a simple dissolved fuel simulant containing only U (~1 M) and Pu (~15 mM) in nitric acid (HNO_3; ~3 M). In FY 2019, two additional flowsheet tests were performed. For the first of these (CoDCon Run 3), the dissolved fuel simulant was similar to that used in the first two tests, with the inclusion of 1 mM neptunium (Np). The second test conducted in FY 2019 (CoDCon Run 4) used a more representative dissolved fuel simulant, including addition of non-radioactive fission product elements. A fifth CoDCon flowsheet test (CoDCon Run 5) was conducted in FY 2020, with the following additional objectives: (1) routing of the technetium (Tc) in the simulated dissolved fuel solution to the solvent extraction raffinate, and (2) routing of the Np in the simulated dissolved fuel solution to the U/Pu product.

All tests used a bank of sixteen 2-cm centrifugal contactors. The tests involved first loading the solvent (30 vol% TBP dissolved in *n*-dodecane) with U and Pu (and Np, for Run 5), then the Pu (and Np) was stripped from the loaded solvent with a U(IV) solution (~50 mM) and the flowsheet conditions were adjusted such that some U partitioned into the Pu-containing product stream. The amount of U accompanying the Pu was monitored in real time using optical spectroscopic techniques coupled with chemometric modeling. Based on the real-time spectroscopic measurement of the U/Pu ratio, adjustments were made to the flowrate of the fresh TBP solvent phase used to scrub U from the aqueous Pu-containing product. This proved to be a very effective way to control the U/Pu mass ratio in the product.

This report presents the results of the CoDCon Run 5 test. The flowsheet tested in Run 5 was substantially different than that run in the prior tests, especially the solvent loading section of the flowsheet. Two key changes were made. First, based on the objective to extract all the Np and route it with the U/Pu product, pentavalent vanadium [V(V)] was added to the feed and scrub solutions. The purpose of the V(V) was to convert all the Np to the +6 oxidation state, which is extractable by TBP. Second, a high acid (8 M HNO_3) scrub was added to the flowsheet to scrub the Tc from the solvent. This was followed by a low acid scrub (0.05 M HNO_3) to reduce the residual HNO_3 concentration in the solvent prior to the Pu stripping step. The output from the low acid scrub was collected separately, rather than routing towards the raffinate.

The modifications to the solvent loading part of the flowsheet were only partially successful. The treatment with V(V) was effective at converting the Np to Np(VI). Only 1.3% of the Np remained in the raffinate solution. However, ~40% of the Np stripped out of the solvent in the low acid scrub step; nearly 20% of the Pu also was stripped from the solvent during the low acid scrub. For further development, either modifications to the flowsheet, or concentration and recycle of the low acid stream into the feed would be required to reduce these losses. The high acid scrub was ineffectual at routing the Tc to the raffinate. Only ~8% of the Tc was in the raffinate solution. Nearly 50% of the Tc entering the process ended up in the Pu-containing product stream.

Uranium(IV) was used to strip the Pu from the TBP solvent. After approximately 90 minutes of the stripping operation, the U/Pu mass ratio stabilized, and remained reasonably stable throughout the remainder of the test (another approximately 330 minutes). Only minor adjustments to the flowrate of the TBP stream used to “re-extract” U in the stripping section was required to maintain the proper U/Pu ratio. Occasional transient drifts of the U/Pu ratio were observed. These were attributed to intrinsic variability in the performance of solvent extraction equipment used. Over the course of the stable operation period, the relative U and Pu fractions in the product were 70.4 ± 0.6 % and 29.6 ± 0.6 %, respectively—well within 1% of the target values.

In summary, the CoDCon project successfully performed five flowsheet tests aimed at producing a U/Pu product with a relative mass ratio of 7/3. With the exception of the first test performed, all tests produced a U/Pu nitrate product with the correct mass ratio within 3%, and in three cases the mass ratio was well within 1% of the target value. The first test missed the target U/Pu ratio because of the chemometric model overpredicting the amount of U(VI) in the product stream. The model was subsequently updated to correct this problem, leading to successful production of the U/Pu product with the correct ratio in the final four flowsheet tests. The project unequivocally demonstrated the utility in optical spectroscopy coupled with chemometric modeling for monitoring and controlling nuclear material process flowsheets. The project resulted in the publication of seven articles in peer-reviewed journals over a 4-year time frame.

CONTENTS

FIGURES

TABLES

ACRONYMS

AMUSE	Argonne Model for Universal Solvent Extraction
CCD	charge-coupled device
CoDCon	co-decontamination
ICP-MS	inductively coupled plasma mass spectrometry
NIR	near infrared
Np	neptunium
PNNL	Pacific Northwest National Laboratory
Pu	plutonium
StDev	standard deviation
TBP	tributyl phosphate
U	uranium
vis	visible (spectral range)

CoDCon PROJECT: FINAL REPORT

1.0 Introduction

The U.S. Department of Energy Office of Nuclear Energy (DOE-NE) tasked Pacific Northwest National Laboratory (PNNL) with testing a co-decontamination (CoDCon) flowsheet for separating a mixed uranium (U)/plutonium (Pu) product from dissolved used nuclear fuel. The primary purpose of the project was to assess, using laboratory-scale equipment, the accuracy and precision to which a specific uranium-to-plutonium (U/Pu) ratio could be achieved in the mixed U/Pu product. For the purpose of this project, the target U/Pu mass ratio was 7/3, as directed by the DOE-NE sponsor. In FY 2020, two additional objectives were pursued: (1) routing the technetium (Tc) in the simulated dissolve fuel solution to the aqueous raffinate stream, and (2) routing the neptunium (Np) in the simulated dissolve fuel solution to the U/Pu product. Integral to this testing effort was demonstrating optical spectroscopic techniques for real-time monitoring of the concentrations of key components, especially U and Pu, in the process solutions. The monitoring capability was essential to achieving the objective of producing a product with a U/Pu mass ratio of 7/3.

The CoDCon flowsheet testing was performed at a scale of nominally 1 kg of U, using simulated dissolved fuel solutions. For the first two flowsheet tests, the dissolved fuel simulant contained only U and Pu dissolved in nitric acid (HNO_3). For the third flowsheet test, Np was added to the simulant. The simulant for the fourth flowsheet test also contained non-radioactive fission product elements. Technetium was added to the simulated dissolved fuel solution for the fifth CoDCon flowsheet test because of the additional testing objective stated above. In all cases, the amounts of metal ions added to the simulated dissolved fuel solution were prototypic of light water reactor fuel burned to ~57,000 GWD/MT.[1]

All the CoDCon tests involved: (1) preparing the surrogate feed solution and associated process solutions, (2) loading the process solvent with U and Pu, (3) reductive stripping of Pu from the solvent, (4) spectroscopic real-time monitoring of all inlet and outlet streams including the U/Pu ratio in the Pu-containing product solution, (5) adjusting the process conditions to achieve the target U/Pu ratio, and (6) off-line analysis of the process solutions. For the first experiment, the U/Pu nitrate product solution was converted to a mixed oxide by modified direct denitration.[2] After runs 2 – 4, the U/Pu nitrate product solution was concentrated and then added to the feed solution for the subsequent run.

The tests were performed using a bank of sixteen 2-cm centrifugal contactors. Because of this limited number of contactors, it was necessary to perform each test in two steps. First, the U and Pu were extracted into an organic solvent consisting of 30 vol% tri-butyl phosphate (TBP) dissolved in *n*-dodecane. During this first part of the experiment, the solvent was scrubbed with a HNO_3 solution to remove any partially co-extracted or entrained material. The resulting loaded solvent was collected and saved for the second part of the experiment. After cleaning out the centrifugal contactor bank, the second half of the experiment was performed, in which the Pu was stripped from the solvent by contacting with a solution of U(IV). The U(IV) reduced the extracted Pu to the poorly extractable +3 oxidation state, thereby causing its transfer to the aqueous phase. This part of the process also included introduction of a fresh TBP solvent stream to “re-extract” U(IV) present in the aqueous phase as it approached the Pu product outlet. The flowrate of this fresh TBP stream was adjusted to allow some U to enter the Pu product so that the target U/Pu ratio could be achieved.

Organic and aqueous input and output streams were monitored in real time by optical spectroscopic techniques. Absorption spectroscopy in the visible (vis) and near-infrared (NIR) regions was applied for determination of actinide species such as Pu(III, IV), U(IV), and Np(V). Raman spectroscopy was used to determine vibrationally active species such as UO_2^{2+} and HNO_3. Although all input[a] and output streams were monitored, focus was placed on monitoring of the U/Pu ratio in the product stream. Chemometric models were used to convert the output of the spectrometers to solution concentrations. This allowed real-time determination of the U/Pu ratio in the solvent extraction product, which was used to inform adjustments as needed to the fresh TBP solvent stream in the U re-extraction stages.. The spectroscopic monitoring approach, and the development of the chemometric models has been described elsewhere.[3]

Two initial CoDCon flowsheet tests were performed in FY 2018.[4] During the first CoDCon flowsheet test, the relative mass fractions of U and Pu in the product were 61% and 39%, respectively. This U/Pu mass ratio was substantially lower than the target value. The low U/Pu ratio was attributed to the chemometric model incorrectly indicating the presence of U(VI) in the product solution, primarily due to an unoptimized calibration transfer between the instruments used to collect the training set and those actually used to monitor the process. Nevertheless, the relative Pu mass fraction was maintained within 3% of the mean value throughout the experiment. Adjustments were made to the chemometric model based on the results of the first test to correct the inaccurate results in the real-time analysis of the process solutions.

A slightly different flowsheet was tested in the second CoDCon run due to a mix up in the aqueous inlet lines. During the second CoDCon flowsheet test, the relative amounts of U and Pu in product solution were initially ~80% and 20%, respectively. However, after adjustments to the flowrate of the TBP solvent phase in the U re-extraction stages of the flowsheet, the target ratio was achieved, and this was maintained over approximately 2.5 h of operation. The U/Pu nitrate solution obtained during this stable period of operation contained 29.3 % Pu and 70.7 % U. This result demonstrated the utility of real-time spectroscopic monitoring in guiding process operations, and also showed that once steady state is achieved, a very stable U/Pu ratio can be maintained.

The third CoDCon flowsheet test was conducted at the end of FY 2018.[5] In this case, the flowsheet tested was the same as in the first test, but Np (1 mM) was added to the aqueous feed solution. Very stable operation of the solvent extraction system was achieved during CoDCon Run 3. The U/Pu ratio was maintained within 1% of the target value for over 5 h of operation. No attempt was made to control the Np behavior during this flowsheet test, and Np was found to split between the raffinate and the U/Pu product. This was explained by Np being in both the extractable Np(VI) form and the poorly extracted Np(V) form in the aqueous feed solution. During the solvent loading step, Np(VI) was transferred to the organic phase along with the U and Pu, while Np(V) remained in the aqueous raffinate. Upon contact of the loaded solvent with U(IV), the Np(VI) was reduced to Np(V) and was therefore transferred to the aqueous phase, along with the Pu(III). The subsequent reduction of Np(V) to Np(IV) (extractable) by U(IV) was sufficiently slow that no appreciable Np(IV) was formed during the relatively short residence time in the centrifugal contactor bank.

A fourth CoDCon flowsheet test was conducted in FY 2019.[5] The flowsheet tested was the same as that used in Runs 1 and 3, but fission product elements (except Tc) were added to the simulated dissolved fuel solution. The addition of zirconium (Zr) to the feed complicated the solvent loading step in that interfacial crud was formed, disrupting the operation. The crud formation was mitigated by adding a small amount of hydrofluoric acid (HF) to the feed solution. The stability of the solvent extraction system during reductive stripping was not as good during Run 4 as it was during Run 3. Although the target U/Pu

---

(a) An exception was the low acid scrub stream applied during the loading step in Run 5; this was not monitored in real time., value was again maintained for over 5 h of operation, the variability around the target value was much greater (~3% around the mean value). It was hypothesized that the drifting of the system observed was due to variability in the ambient temperature in the laboratory space during the course of the run, but this hypothesis has not been verified. The Np behavior during Run 4 was similar to that for Run 3.

In this report we describe the results of the fifth CoDCon flowsheet test and discuss these results in the context of the results of the prior tests. The flowsheet tested in CoDCon Run 5 was modified to achieve the objectives of (a) routing Tc to the raffinate and (b) routing all Np to the U/Pu product. The changes to the flowsheet were in the solvent loading section. The approach in developing the revised flowsheet was to maintain the loaded solvent composition as close as possible to that in the previous tests. This approach was taken to minimize perturbations to the reductive stripping section of the flowsheet, so that control of the U/Pu ratio was much the same as in the previous four runs. Figure 1.1 shows the flowsheet tested in Run 5, and Table 1.1 describes the labeling of the various process streams. In order to force Tc into the aqueous raffinate (stream *A4*), a high HNO_3 scrub was added to the flowsheet. Following 8 extraction stages, 6 stages of 8 HNO_3 scrubbing of the solvent was performed to remove the Tc from the solvent. The high HNO_3 scrub resulted in a HNO_3 in the organic phase greater than that in the loaded solvent from previous CoDCon tests. To lower the organic phase HNO_3 concentration, two stages of scrubbing with 0.05 M HNO_3 were implemented. The aqueous outlet from this second scrubbing step was collected separately (stream *A5*) and was not counter-currently fed to the lower contactor stages. The reductive stripping portion of the flowsheet was essentially identical to that implemented in Runs 1, 3, and 4.

In order to route all of the Np to the U/Pu product, vanadium(V) was added to the feed solution to oxidize the Np to Np(VI),[6-7] so that the Np could be completely extracted by TBP. Vanadium(V) was also added to the 8 M HNO_3 and 0.05 M HNO_3 scrub solutions to maintain Np(VI) during scrubbing of the loaded solvent. Although, as discussed later in this report, complete maintenance of Np(VI) during the 0.05 M HNO_3 scrub was not achieved, resulting in substantial loss of Np to the low-acid scrub outlet stream.

This report fulfills milestone number M2FT-20PN0304010313 in the U.S. Department of Energy Office of Nuclear Energy Nuclear Technology Research and Development Program.

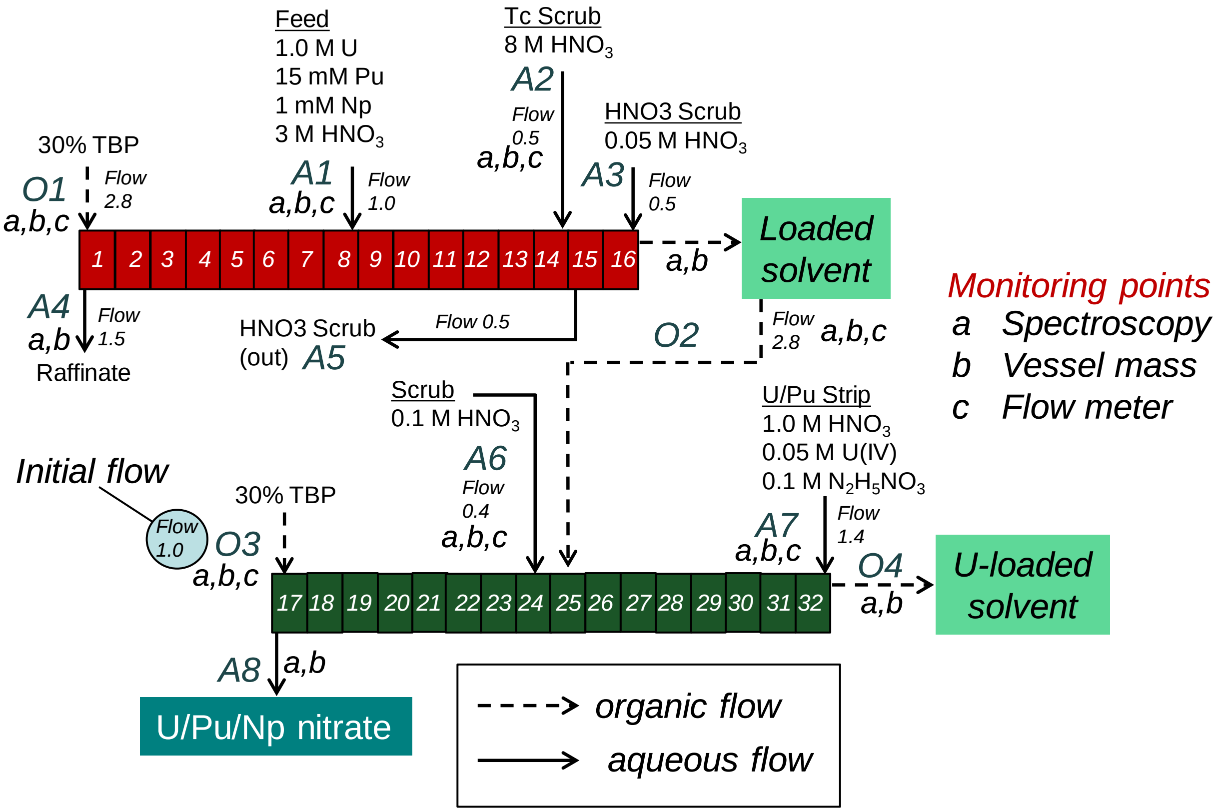

Figure 1.1. CoDCon flowsheet tested in Run 5.

Table 1.1. Description and labels for the process streams in the CoDCon solvent extraction flowsheet.

Process stream label	***Description***
A1	Aqueous dissolved fuel simulant feed
A2	8 M HNO_3 Tc scrubbing solution; with 10 mM V(V)
A3	0.05 M HNO_3 solution for scrubbing HNO_3 from the solvent; with 10 mM V(V)
A4	Aqueous raffinate for solvent loading step
A5	Outlet from 0.1 M HNO_3 solvent scrub
A6	0.1 M HNO_3 scrub solution for U/Pu stripping step
A7	Aqueous U(IV) solution used as Pu and Np reductant
A8	U/Pu/Np nitrate product stream
O1	Fresh TBP solvent for U/Pu loading
O2	U/Pu-loaded TBP solvent
O3	Fresh TBP solvent for U re-extraction
O4	Pu-depleted TBP solvent

2.0 Experimental

2.1 Equipment

The equipment used in the CoDCon flowsheet tests has previously been described in detail,[1, 4] so only the key features of the testing system are summarized here. The solvent extraction was performed in 2-cm centrifugal contactors fabricated at Argonne National Laboratory.[8] A bank of 16 stages of the 2-cm centrifugal contactors was used. Metering pumps with variable speed controllers were used to feed the process solutions to the contactor bank. The pump flowrates were calibrated with the specific solutions used by determining the mass of solution passed over known time intervals at selected pump settings. The densities of the solutions involved were used to convert the masses collected to volumes for determining flowrates in terms of milliliters per minute (mL/min). Linear calibration lines for the flowrate versus pump setting were generated. Pulse dampeners and filters were installed between the pumps and the contactor bank.

The solvent extraction system was equipped with on-line optical spectroscopy. All spectroscopic equipment was procured from Spectra Solutions (Norwood, MA). Quartz flow-through cells (1-cm path length) were held within machined cell holders as previously described.[1, 4] Visible (vis) absorption, near infrared (NIR) absorption, and Raman spectroscopies were applied to monitor the process solutions. The visible spectral region primarily provided data relevant to the concentrations of Pu(III, IV, and VI) and U(IV); the NIR spectrometer allowed the determination of Np(V,VI) in the process solutions; and the Raman spectrometer was the primary source of data relevant to the U(VI) and HNO_3 concentrations. While the Raman and vis spectrometers utilized CCD cameras capable of simultaneous measurement of 6 flow cells, the NIR CCD detector was limited to single channel interrogation. The NIR therefore required the use of a motorized multiplexor that allowed sequential measurement of the 6 flow cells. The NIR was added to the system by bifurcating collection fibers to split signal between the vis and NIR instruments. The NIR excitation signal was prefabricated into the vis excitation source and allowed for the two systems to use the same source and excitation fibers.

2.2 Preparation of the Dissolved Fuel Simulant

Most of the components of the dissolved fuel simulant were added as the nitrate salts. Table 2.1 lists the non-radioactive components used to make up the simulant, along with the quantities used to prepare 4.2 L of dissolved fuel simulant. Except for tin (Sn) and Zr, each nitrate salt was added to a 1 M HNO_3 solution (~1 L) and dissolved by mixing. Tin metal was dissolved separately in 1 M HNO_3 at ambient temperature. Zirconyl nitrate was also dissolved separately in 1 M HNO_3. The separate Sn and Zr solutions were added to the main solution (total volume ~1.1 L at this point) and the mixture was stirred for one week. The mixture was centrifuged to separate the liquid from the bulk of the undissolved solids, then the liquid phase was filtered through a 0.45-µm polyethersulfone (PES) membrane (Nalgene™ Rapid-Flow™ Sterile Disposable Filter Unit). The HNO_3 concentration in the resulting solution was determined to be 0.85 ± 0.01 M by titration with standard NaOH.

The uranyl nitrate solution was prepared by dissolving various in-house stocks of depleted uranium oxides (UO_2 or UO_3) in HNO_3. After filtering, the U(VI) concentration was determined to be 1.94 M and the HNO_3 was estimated to be 0.27 M. The U concentration was determined spectrophotometrically. The HNO_3 concentration was determined by measuring the solution density (1.6286 g/cm^3 at 21 °C) and applying the equation of Burger as reported by Sakurai et al.[9] Concentrated HNO_3 (14.3 M; 440 mL) was added to a 4-L Pyrex beaker followed by addition of 2.09 L of the 1.94 M U stock solution. The solution was stirred at 200 RPM with a Teflon coated stir bar until homogenous. The non-radioactive portion of the simulant (1.1 L) was then added. The solution was stirred at 200 RPM for 19 hours. A very small amount of solid was observed on the surface of the solution, but the bulk of the solution showed no evidence of light scattering when exposed to a handheld laser pointer. The solution was filtered through a 0.45 µm PES filter and was then transferred into a radiological glovebox for introduction of the Pu and Np stock solutions. Most of the Np and Pu used was from the concentrated product from Run 4 (~575 mL; 6.48 M HNO_3).[5] After addition of the Run 4 concentrated product, the concentrations of Pu, U, and Np in the mixture were determined spectrophotometrically, and additional Pu and Np from in-house stocks were added to reach the target concentrations of ~15 mM Pu and ~1 mM Np. The composition of the dissolved fuel simulant is discussed in Section 3.1.

The U(IV) solution used in the stripping portion of the test was prepared by electrochemical reduction of U(VI), as previously described.[2] Tributyl phosphate was obtained from Aldrich, *n*-dodecane was obtained from Alfa Aesar, HNO_3 was obtained from Fisher, and aqueous hydrazine (N_2H_4) (35 wt%) was obtained from Acros Organics. Before use, the hydrazine was neutralized with HNO_3 while cooling in an ice water bath to form $N_2H_5NO_3$.

Table 2.1. Amounts of the non-actinide components used in preparing 4.2 L of CoDCon Run 5 feed simulant.

Formula	*Mass (g)*	*Manufacturer*	*Lot #*
$Ce(NO)_3 \cdot 6H_2O$	14.513	Acros Organics	A0385618
$Cr(NO_3)_3 \cdot 9H_2O$	48.542	Aldrich	02808PG
$CsNO_3$	7.437	Aldrich	MKCG3297
$Eu(NO)_3 \cdot 6H_2O$	0.967	Alfa Aesar	Q20C039
$Fe(NO)_3 \cdot 9H_2O$	102.196	Sigma Aldrich	MKCG1626
$Gd(NO)_3 \cdot 6H_2O$	0.940	Research Chemicals	GD-N-3-009
$La(NO)_3 \cdot 6H_2O$	8.259	American Potash and Chemical Corp	S28 R1208
$Na_2MoO_4 \cdot 2H_2O$	5.992	Sigma	30K0210
$Nd((NO)_3 \cdot 6H_2O$	23.954	Aldrich	MKCK4638
$Ni(NO)_2 \cdot 6H_2O$	53.847	Sigma Aldrich	BCBV6886
102 mg/mL Pd sol’n	0.297 (mL)	In-house stock	Not applicable
$Pr(NO)_3 \cdot 6H_2O$	6.614	Alfa Aesar	K24U008
$RbNO_3$	0.767	Acros Organics	A0330127
$Ru(NO)(NO)_3$ sol’n (112 g/L)	20.2 (mL)	In-house stock	Not applicable
$Sm(NO)_3 \cdot 6H_2O$	5.036	Research Chemicals	Sm-N-3-018
Sn metal	0.109	J.T. Baker	25281
$Sr(NO_3)_2$	3.702	In-house stock	Not applicable
$Na_2TeO_4 \cdot 2H_2O$	1.002	Unmarked	Unmarked
$Y(NO)_3 \cdot 6H_2O$	3.704	Research Chemicals	Y-N-3-044
$ZrO(NO_3)_2 \cdot xH_2O$	18.726	Alfa Aesar	43224

2.3 Solvent Extraction

2.3.1 Batch Contacts

Two sets of batch contacts were performed to verify extraction of Np. Both sets were conducted in similar manner, but one was done immediately after adding V(V) to an aliquot of the feed solution (taken before Tc addition), while the other was done 24 h after the V(V) addition to the feed. Vanadium pentoxide (V_2O_5, 9.1 mg) was added to 10 mL of the feed solution to give a V concentration of 10 mM. This was done to convert Np in solution to the extractable +6 oxidation state. Duplicate aliquots of the adjusted feed solution (1 mL) were mixed with 0.5 mL of 8 M HNO_3 that also contained 10 mM V(V) (this represented the high acid scrub solution, stream A2 in Figure 1.1). These samples were saved for analysis by absorption spectroscopy. Another set of duplicate aliquots of the adjusted feed solution (1 mL) was mixed with 0.5 mL of 8 M HNO_3/10 mM V(V) solution. The latter aliquots were each contacted with 2.8 mL of 30% TBP in *n*-dodecane by vortex mixing for 10 minutes. The mixtures were centrifuged to aid in phase disengagement, then the organic phases were separated. After removing a 0.3-mL aliquot from each aqueous phase for analysis, the remaining aqueous solutions were contacted with 2.24 mL of fresh 30% TBP in the same manner as above. Aliquots of the aqueous and organic phases from each contact were analyzed for Np by absorption spectroscopy (both in the visible and NIR regions).

2.3.2 Solvent Loading

Approximately 24 hours prior to commencement of the solvent loading step, V_2O_5 (3.8 g) was added to the simulated dissolved fuel solution (4.2 L) to give 10 mM V(V) in the feed solution to adjust the Np valence to +6.(a) The system was started in the following sequence.

1. 0.1 M HNO_3 was pumped to stage 16 at a rate of 10 mL/min; the flowrate was decreased to a target value of 5 mL/min when aqueous solution was observed to exit at stage 14.

2. 0.1 M HNO_3 was pumped to stage 13; upon exiting at stage 1, this solution was used to baseline the on-line spectroscopic equipment to be used to monitor the composition of the aqueous raffinate.

3. 30% TBP was pumped to stage 1 at a rate of 20 mL/min; once the organic phase was observed to exit stage 16, the 30% TBP flowrate was adjusted to 28 mL/min.

4. The spectroscopic baseline was obtained on the organic phase outlet at stage 16.

5. 8 M HNO_3 containing 10 mM V(V) was pumped to stage 14 at a target flow rate of 5 mL/min.

6. 0.05 M HNO_3 containing 10 mM V(V) was pumped to stage 16 at a target flow rate of 5 mL/min.

7. The simulated dissolved fuel feed solution was pumped to stage 8 at a target flow rate of 10 mL/min.

The system was run until all the aqueous feed solution had been processed. During the loading run, timed grab samples were periodically taken from the aqueous outlet from stage 1, and from the organic outlet of stage 16. The mass was measured and recorded for each grab sample so that flowrates could be calculated. Periodic measurements were made for the mass of the vessels containing the 30% TBP solvent, the loaded solvent, the aqueous feed solution, the 0.05 M HNO_3 scrub solution, and the 8 M HNO_3 scrub solution. The balances used for the latter measurements were not calibrated, so the reported values are for indication only. Also, throughout the loading step, the compositions of the various input and output streams were tracked using the on-line spectroscopic monitoring system.

Upon completion of the loading step, the contactor bank was flushed with 0.1 M HNO_3 and *n*-dodecane until the spectroscopic monitor indicated no metal ions present in the exit streams. The system was then flushed with deionized water to remove HNO_3 from the system.

(a) After the solvent loading step was completed, it was discovered that there was some undissolved V_2O_5 on the bottom of the feed vessel. So, presumably the V(V) concentration was somewhat less than 10 mM.

2.3.3 Reductive Stripping

The U(IV) solution used to strip the Pu from the loaded solvent was prepared electrolytically as previously described.[2] The system was started up in the following sequence for the stripping portion of the test.

1. 0.1 M HNO_3 was pumped into stage 24 (contactor 8) and stage 32 (contactor 16).
2. The aqueous spectral baseline was recorded.
3. After aqueous solution was seen exiting stage 17 (contactor 1), the flow of fresh 30% TBP was started at stage 17 (contactor 1).
4. The flowrate for the 0.1 M HNO_3 scrub at stage 24 (contactor 8) was set to a target value of 4 mL/min.
5. To establish the organic phase spectral baseline, fresh 30% TBP was passed through the spectral flow-through cell at stage 25 (contactor 9).
6. After organic phase was observed to exit at stage 32 (contactor 16), the fresh 30% TBP flowrate at stage 17 (contactor 1) was adjusted to 10 mL/min, and the spectral baseline at the stage 32 (contactor 16) organic outlet was established.
7. The U(IV) solution was introduced into stage 32 (contactor 16) at a flowrate of 14 mL/min.
8. After flowing the U(IV) solution for ~15 min, the loaded TBP solvent was pumped to stage 25 (contactor 9) at a target flow rate of 28 mL/min.

Similar to the loading step, timed grab samples were periodically taken of the aqueous and organic outlets, and mass measurements were performed on the various process vessels (for indication only). The aqueous U/Pu/Np product was collected into a series of 1-L poly bottles. Adjustments were made to the flowrate of the fresh 30% TBP solvent at stage 17, based on the U/Pu ratio indicated by the on-line spectroscopic monitor. The system was operated until the U(IV) solution was completely consumed. At the conclusion of the test, the contents of each contactor were collected. The volumes of aqueous and organic phase drained from each contactor were estimated by comparing the volumes against a graduated vial of the same geometry as those used to collect the contactor contents. Due to resource constraints, the samples taken from the contactors at the conclusion of the test were not analyzed.

After the test, the contactor bank was cleaned out in a manner similar to that described in Section 2.3.2.

2.3.4 Analytical Methods

The vis and NIR absorption spectrometers, and the Raman spectrometer, used for online monitoring were procured from Spectra Solutions, Inc. This equipment has been described in detail elsewhere.[3] Off-line vis absorption spectroscopy was performed using a single beam Spectral Instruments model 420 CCD array detector spectrophotometer with a 350−950 nm scanning range, 1.2 nm spectral bandwidth, and 1.2 nm wavelength accuracy. Nitric acid concentrations were determined by titration with standard NaOH using a Metrohm 905 Titrando platform with an 800 Dosino pump and a Metrohm 804 Ti stand for stirring. Ammonium oxalate (0.2 M) was added to the samples before titration to complex metal ions.[10]

Metal ion concentrations were determined by inductively coupled plasma mass spectrometry (ICP-MS) using a Perkin Elmer - Model: NexION 350x with a HF-Resistant Sample Introduction Kit with Sapphire Injector.

3.0 Results

This section describes the experimental results. First, the composition of the simulated dissolved fuel solution is presented. This is followed by the results of the preliminary batch contacts performed to verify Np extraction. Finally, the results of the fifth CoDCon flowsheet test are presented, including a comparison between the experimental results and predictions made through modeling of the flowsheet using the Argonne Model for Universal Solvent Extraction (AMUSE) code.

3.1 Composition of Simulated Dissolved Fuel Solution

Table 3.1 presents the composition of the dissolved fuel simulant. The table presents the target concentration of each component, along with the values obtained for those components that were experimentally measured. For most components, the measured concentrations were in line with the target values. Tin was an exception—this element was not detected by ICP-MS (detection limit of 2×10^{-7} M) indicating its precipitation during preparation of the simulant. Actual concentration of Zr was below the target suggesting its possible precipitation as well.

3.2 Batch Contacts

Before performing the counter-current flowsheet test, batch solvent extraction contacts were performed to verify Np extraction under the expected flowsheet conditions. Pentavalent vanadium [V(V)] was added to both the feed solution and the 8 M HNO_3 scrub solution at a concentration of 10 mM. The function of the V(V) was to adjust the Np to the extractable NpO_2^{2+} form.[6] The V(V)-adjusted feed solution and 8 M HNO_3 scrub solution were mixed together in a 2:1 ratio to mimic the mixing of these streams that would occur during the solvent loading part of the flowsheet test. Two successive contacts with 30% TBP (organic-to-aqueous ratio of 2.8/1.5) were conducted both immediately after V(V) addition, and 24 h after V(V) addition. No significant difference was observed between the immediately performed contacts and those performed after the 24-h waiting period.

Before treatment with V(V), the total Np concentration in the feed solution was determined to be 1.11 mM. Adjusting for dilution with the scrub solution, the initial Np concentration in the aqueous phase for the batch contacts was 0.74 mM. Spectral analysis of the aqueous phase before contacting with TBP indicated incomplete conversion of Np to the +6 state. Rather, the solution contained 73% Np(VI) and 27% Np(V).[a] The mixture of Np(V) and Np(VI) can be explained by the establishment of the following equilibrium:[11]

$$NpO_2^{+} + VO_2^{+} + 2H^{+} \rightleftharpoons NpO_2^{2+} + VO^{2+} + H_2O \qquad (3.1)$$

After performing the two successive batch extraction contacts, the Np concentration in the aqueous phase was 3.6×10^{-3} mM. Thus, 99.5% of the Np was extracted in the two batch contacts. The near quantitative Np extraction can be explained by the driving of reaction 3.1 to the right upon extraction of NpO_2^{2+} into

---

[a] These percentages of Np species assumes that no Np(IV) is present in the solution. The presence of Np(IV) is difficult to detect because of spectral interferences from Pu(IV), Pu(VI), and the non-radioactive fission product surrogates present in the feed solution.

the organic phase. This result gave confidence that effective extraction of Np could be achieved in the CoDCon flowsheet by application of V(V).

Table 3.1. Composition of the dissolved fuel simulant used in CoDCon Run 5.

Component	***Target Conc., mol/L***	***Measured Conc., mol/L***[(a)]
Ce	8.0×10^{-3}	7.95×10^{-3}
Cr	2.9×10^{-2}	(b)
Cs	9.1×10^{-3}	9.15×10^{-3}
Eu	4.4×10^{-4}	5.21×10^{-4}
Fe	6.0×10^{-2}	(b)
Gd	4.9×10^{-4}	9.14×10^{-4}
La	4.1×10^{-3}	4.56×10^{-3}
Mo	5.8×10^{-3}	4.33×10^{-3}
Nd	1.3×10^{-2}	1.17×10^{-2}
Ni	4.3×10^{-2}	(b)
Pd	6.8×10^{-5}	1.50×10^{-4}
Pr	3.6×10^{-3}	3.64×10^{-3}
Rb	1.2×10^{-3}	1.37×10^{-3}
Ru	5.3×10^{-3}	5.17×10^{-3}
Sm	2.4×10^{-3}	2.60×10^{-3}
Sn	2.0×10^{-4}	(c)
Sr	4.1×10^{-3}	4.58×10^{-3}
Te	8.6×10^{-4}	7.41×10^{-4}
Y	2.3×10^{-3}	(b)
Zr	1.9×10^{-2}	9.93×10^{-3}
U	1.0×10^{0}	1.10×10^{0}
Np	1.0×10^{-3}	1.22×10^{-3}
Pu	1.5×10^{-2}	1.46×10^{-2}
Tc	1.8×10^{-3}	2.07×10^{-3}
HNO_3	3.0×10^{0}	2.69×10^{0} (d)

(a) Determined by ICP-MS, unless otherwise noted

(b) Not measured

(c) Below the detection limit

(d) Determined by titration

3.3 CoDCon Run 5

This section presents the results of the fifth CoDCon flowsheet test (Run 5). The results are organized in the following manner. First, the flowrates of the various process streams achieved during the test are compared against the planned flowrates. Second, the compositions of the different process streams are discussed, along with the distribution of the simulated fuel components across the various process streams. Third, the U/Pu ratio in Pu-containing product is evaluated over the course of the experiment.

3.3.1 Evaluation of Flowsheet Execution

The flowsheet tested in Run 5 is shown in Figure 1.1. The target flowrate for each process stream is presented in Table 3.2 along with the measured values determined by (a) changes in the mass of the various process vessels (including the U/Pu product collection bottles), (b) timed grab samples, and (c) output from the flow meters. The relatively large standard deviations in the flow meter data are due to transient spikes in the flow meter readings. Generally, there was good agreement between the flowrates determined by the different techniques. The measured flowrates were mostly close to the target values; however, for streams with relatively low flowrates (the scrub streams), the measured values tended to be lower than the target values. The flow of the raffinate stream (*A4*) was ~15% lower than what would be expected by summing of the *A1* and *A2* aqueous streams. This might be attributable to mass transfer of U and Pu to the organic phase, but could also be due to uncertainty in the flowrate measurements. Similarly, the measured flowrate for the Pu-depleted solvent stream (*O4*) was less than that expected base on the sum of the input organic streams (*O2* + *O3*).

Table 3.2. Target and measured flowrates (in mL/min) for CoDCon Run 5.

Process stream	***Target***	***Measured by***		
		Vessel masses(a)	***Grab samples***	***Flow meter***
A1	10.0	10.7 ± 0.5	NA	10.91.3 ± 3.2
A2	5.0	4.5 ± 0.2	NA	3.4 ± 1.5
A3	5.0	4.2 ± 0.2	NA	NA
A4	15.0(b)	12.6 ± 1.8	13.2 ± 0.2	NA
A5	5.0	4.1 ± 0.1	4.0 ± 0.7	NA
A6	4.0	3.0 ± 0.2	NA	2.6 ± 0.5
A7	14.0	14.9 ± 0.5	NA	15.4 ± 2.2
A8	18.0(b)	16.7 ± 0.7	16.5 ± 0.3	NA
O1	28.0	27.9 ± 1.5	NA	31.7 ± 1.3
O2(c)	28.0	27.8 ± 1.0	28.4 ± 1.8	NA
O2(d)	28.0	25.7 ± 1.9	NA	27.9 ± 2.4
O3	10.0(e)	10.6 ± 0.8(f)	NA	11.3 ± 0.7
O4	38.0(b,e)	35.2 ± 2.2	33.2 ± 1.2	NA

(a) Flowrates determined from vessel masses are for indication only.
(b) Assumes flowrates of input streams are additive.
(c) Loaded solvent flow during loading step.
(d) Loaded solvent flow during stripping step.
(e) Initial target value for flow of fresh TBP stream to stage 17.
(f) Average flow over the course of the stripping step; adjustments were made during this time to achieve the desired U/Pu ratio. The mean value during stable product output (≥ 90 minutes) was 10.8 ± 0.6 mL/min (vessel masses) or 11.4 ± 0.5 mL/min (flow meter).
NA = not applicable

3.3.2 Solution Compositions and Fuel Component Distributions

The detailed composition of the aqueous feed solution for Run 5 is given in Table 3.1. The key components of the other process input streams are summarized in Table 3.3. In the following subsections, the behavior of selected feed components during the process are discussed.

Table 3.3. Actinide and HNO_3 concentrations in the process input streams for Run 5.

Stream #	***Description***	***HNO_3, M***	***U(VI), mM***	***U(IV), mM***	***Pu, mM***	***Np, mM***
A1	Feed[(a)]	2.69 ± 0.01	1100	NA	14.6	1.22
A2	8 M HNO_3	7.87 ± 0.01	NA	NA	NA	NA
A3	0.05 M HNO_3	0.0520 ± 0.0004	NA	NA	NA	NA
A6	0.1 M HNO_3	0.109 ± 0.002	NA	NA	NA	NA
A7	U(IV)[(b)]	1.08 ± 0.01	4.4	48.5	NA	NA

[(a)] Actinides determined by ICP-MS; uncertainties are estimated to be 15%
[(b)] Uranium species determined by vis spectroscopy
NA = not applicable

3.3.2.1 Uranium

Table 3.4 presents the distribution of U during the solvent loading step, based on the U analysis by ICP-MS. Uranium recovery between the low-acid scrub bottles (*A5*), the raffinate (*A4*), and the loaded solvent (*O2*) was 92%, given the amount of U measured to be in the feed solution. As expected, very little of the U was found in the raffinate solution. Approximately 6% of the U was found in the low-acid scrub output solution.

Table 3.5 presents the distribution of U during the Pu stripping step. Uranium entered this section of the flowsheet through two streams—the loaded solvent (*O2*) and the U(IV) stripping solution (*A7*). As intended, 97% of the U was retained in the solvent during Pu stripping, with the remaining 3% reporting to the U/Pu/Np product stream. The U recovery during the stripping portion of the test was 95%.

Table 3.4. Uranium behavior during the solvent loading step.

Process Stream	***Vol., L***	***[U], mol/L***	***Mass U, g***	***Percent U***[a]
Feed (*A1*)	4.05	1.10×10^{0}	1.06×10^{3}	
Low acid scrub bottle 1 (*A5*)	0.85	1.75×10^{-1}	3.54×10^{1}	3.6
Low acid scrub bottle 2 (*A5*)	0.67	1.48×10^{-1}	2.36×10^{1}	2.4
Raffinate (*A4*)	4.76	1.89×10^{-5}	2.14×10^{-2}	0.0
Loaded solvent (*O2*)	11.00	3.51×10^{-1}	9.18×10^{2}	94.0
U Recovered			9.77×10^{2}	
Recovery, %			92%	

(a) Percentage based on the total U recovered in the scrub bottles, raffinate, and loaded solvent.

Table 3.5. Uranium behavior during the Pu stripping step.

Process Stream	***Vol, L***	***[U], mol/L***	***Mass U, g***	***Percent U***[a]
Loaded solvent (*O2*)	10.62	3.51×10^{-1}	8.86×10^{2}	
U(IV) solution (*A7*)	6.17	5.29×10^{-2} [b]	7.77×10^{1}	
Product bottle 1 (*A8*)	0.87	1.14×10^{-2}	2.35×10^{0}	0.3
Product bottle 2 (*A8*)	0.87	1.95×10^{-2}	4.03×10^{0}	0.4
Product bottle 3 (*A8*)	0.89	1.68×10^{-2}	3.56×10^{0}	0.4
Product bottle 4 (*A8*)	0.97	1.79×10^{-2}	4.14×10^{0}	0.5
Product bottle 5 (*A8*)	0.97	1.72×10^{-2}	3.95×10^{0}	0.4
Product bottle 6 (*A8*)	0.90	1.57×10^{-2}	3.35×10^{0}	0.4
Product bottle 7 (*A8*)	0.91	1.55×10^{-2}	3.36×10^{0}	0.4
Product bottle 8 (*A8*)	0.62	1.53×10^{-2}	2.27×10^{0}	0.2
Pu-Depleted Solvent (*O4*)	14.67	2.56×10^{-1}	8.92×10^{2}	97.1
U Recovered			9.19×10^{2}	
Recovery, %			95%	

(a) Percentage based on the total U recovered in the product bottles and the Pu-depleted solvent.

(b) The U concentration in the U(IV) solution was determined by vis absorption spectroscopy, all others were determined by ICP-MS.

3.3.2.2 Plutonium

Table 3.6 presents the distribution of Pu during the solvent loading step. Plutonium recovery between the low-acid scrub bottles (*A5*), the raffinate (*A4*), and the loaded solvent (*O2*) was 93%, which is similar to what was determined for U (Table 3.4). The Pu concentration in the raffinate solution was very low, representing < 0.05% of the Pu in the feed solution. A substantial fraction of the Pu (18%) was found in the low-acid scrub solutions. For an industrial application of CoDCon, this low-acid scrub stream would need to be recycled back to the feed solution to minimize the loss of Pu, or the flowsheet would need to be modified.

Table 3.7 presents the distribution of Pu during the Pu stripping step. Good stripping of Pu was achieved, with the Pu remaining in the Pu-depleted solvent below the ICP-MS detection limit. Plutonium mass recovery was 107% during this portion of the flowsheet, based on the amount of Pu entering in the loaded solvent stream.

Table 3.6. Plutonium behavior during the solvent loading step.

Process Stream	***Vol., L***	***[Pu], mol/L***	***Mass Pu, g***	***Percent Pu***[(a)]
Feed (*A1*)	4.05	1.46×10^{-2}	14.2×10^{1}	
Low acid scrub bottle 1 (*A5*)	0.85	6.93×10^{-3}	1.41×10^{0}	10.7
Low acid scrub bottle 2 (*A5*)	0.67	5.96×10^{-3}	9.54×10^{-1}	7.3
Raffinate (*A4*)	4.76	1.22×10^{-6}	1.39×10^{-3}	0.0
Loaded solvent (*O2*)	11.00	4.09×10^{-3}	1.08×10^{1}	82.0
Pu Recovered			1.31×10^{1}	
Recovery, %			93%	

(a) Percentage based on the total Pu recovered in the scrub bottles, raffinate, and loaded solvent.

Table 3.7. Plutonium behavior during the Pu stripping step.

Process Stream	***Vol, L***	***[Pu], mol/L***	***Mass Pu, g***	***Percent Pu***[a]
Loaded solvent (*O2*)	10.62	4.09×10^{-3}	1.04×10^{1}	
Product bottle 1 (*A8*)	0.87	4.51×10^{-3}	9.38×10^{-1}	8.4
Product bottle 2 (*A8*)	0.87	7.42×10^{-3}	1.24×10^{0}	13.8
Product bottle 3 (*A8*)	0.89	7.28×10^{-3}	1.57×10^{0}	14.0
Product bottle 4 (*A8*)	0.97	7.28×10^{-3}	1.69×10^{0}	15.2
Product bottle 5 (*A8*)	0.97	6.89×10^{-3}	1.63×10^{0}	14.3
Product bottle 6 (*A8*)	0.90	6.61×10^{-3}	1.45×10^{0}	12.7
Product bottle 7 (*A8*)	0.91	6.62×10^{-3}	1.44×10^{0}	13.0
Product bottle 8 (*A8*)	0.62	6.46×10^{-3}	9.75×10^{-1}	8.6
Pu-Depleted Solvent (*O4*)	14.67	Not detected	Not detected	0.0
Pu Recovered			1.11×10^{1}	
Recovery, %			107%	

[a] Percentage based on the total Pu recovered in the product bottles and the Pu-depleted solvent.

3.3.2.3 Neptunium

Routing of Np to the Pu stripping stream (*A8*) to form a mixed U/Pu/Np product was a specific objective of the CoDCon Run 5 test. Table 3.8 presents the distribution of Np during the solvent loading step. Pentavalent vanadium was added to the feed solution and the scrubs solutions to convert the Np to the extractable +6 oxidation state. The results indicate that this method was mostly effective, with only 1.2% of the Np remaining in the aqueous raffinate solution. Additional extraction stages would presumably result in even lower loss of Np to the raffinate. As was the case with Pu, a substantial fraction of the Np (39.2%) was found in the low-acid scrub solutions. (see Section 3.4 and Appendix A for further discussion). Again, this low-acid scrub stream would need to be recycled back to the feed solution to minimize the loss of Np and Pu, or further modification to the flowsheet would be required for industrial application. Mass recovery of Np was 89% during the solvent loading step, similar to that achieved for U and Pu.

Table 3.9 presents the distribution of Np during the Pu stripping step. Based on the results of previous CoDCon runs,[4-5] it was expected that essentially quantitative stripping of Np from the solvent would occur during this test through the reduction of the extracted Np(VI) to the poorly extracted Np(V) by U(IV). This was indeed the case, with Np being below detection by ICP-MS in the Pu-depleted solvent. Mass recovery was 99% for Np in the Pu stripping portion of the experiment.

Table 3.8. Neptunium behavior during the solvent loading step.

Process Stream	***Vol., L***	***[Np], mol/L***	***Mass Np, g***	***Percent Np***(a)
Feed (*A1*)	4.05	1.22×10^{-3}	1.17×10^{0}	
Low acid scrub bottle 1 (*A5*)	0.85	1.16×10^{-3}	2.34×10^{-1}	22.4
Low acid scrub bottle 2 (*A5*)	0.67	1.10×10^{-3}	1.75×10^{-1}	16.8
Raffinate (*A4*)	4.76	1.19×10^{-5}	1.34×10^{-2}	1.2
Loaded solvent (*O2*)	11.00	2.39×10^{-4}	6.22×10^{-1}	59.6
Np Recovered			1.04×10^{0}	
Recovery, %			89%	

(a) Percentage based on the total Np recovered in the scrub bottles, raffinate, and loaded solvent.

Table 3.9. Neptunium behavior during the Pu stripping step.

Process Stream	***Vol, L***	***[Np], mol/L***	***Mass Np, g***	***Percent Np***(a)
Loaded solvent (*O2*)	10.62	2.39×10^{-4}	6.00×10^{-1}	
Product bottle 1 (*A8*)	0.87	2.52×10^{-4}	5.19×10^{-2}	8.8
Product bottle 2 (*A8*)	0.87	3.62×10^{-4}	7.45×10^{-2}	12.6
Product bottle 3 (*A8*)	0.89	3.85×10^{-4}	8.14×10^{-2}	13.8
Product bottle 4 (*A8*)	0.97	3.95×10^{-4}	9.07×10^{-2}	15.3
Product bottle 5 (*A8*)	0.97	3.77×10^{-4}	8.63×10^{-2}	14.6
Product bottle 6 (*A8*)	0.90	3.61×10^{-4}	7.67×10^{-2}	13.0
Product bottle 7 (*A8*)	0.91	3.61×10^{-4}	7.79×10^{-2}	13.2
Product bottle 8 (*A8*)	0.62	3.56×10^{-4}	5.26×10^{-2}	8.9
Pu-Depleted Solvent (*O4*)	14.67	Not detected	Not detected	0.0
U Recovered			5.92×10^{-1}	
Recovery, %			99%	

(a) Percentage based on the total Np recovered in the product bottles and the Pu-depleted solvent.

3.3.2.4 Technetium

Exploration of Tc management in the CoDCon flowsheet was a new objective of the CoDCon Run 5 test. Table 3.10 summarizes the behavior of Tc during the solvent loading part of the test. The 8 M HNO_3 scrub was added to the flowsheet to direct the Tc to the aqueous raffinate stream (*A4*), however, the results indicate that this was ineffective. Although the Tc concentration in the raffinate could not be accurately determined by ICP-MS because of isobaric interferences (primarily from ^{99}Ru), it is estimated that only ~8% of the Tc reported to the raffinate solution, based on the amounts of Tc measured to be in the feed solution, the two low-acid scrub bottles (stream *A5*), and the loaded solvent.(a) Approximately 72% of the Tc remained in the loaded solvent.

Table 3.11 presents the Tc distribution during the reductive stripping portion of the Run 5 test. The total amount of Tc found in the eight product bottles was 0.399 g and that found in the Pu-depleted solvent was 0.189 g, for a total of 0.587 g Tc. Given that 0.580 g Tc was present in the volume of loaded solvent that was processed, this represented a 101% recovery of Tc during the reductive stripping step. Based on the total output of 0.587 g, 68% of the Tc entering the reductive stripping section of the flowsheet was in the U/Pu/Np product, while 32% remained in the Pu-depleted solvent (remaining with the bulk U). Since 72% of the total Tc entering into the process via the feed was in the loaded solvent, approximately 50% of the Tc in the feed ended up in the U/Pu/Np product.

Table 3.10. Technetium behavior during the solvent loading step.

Process Stream	***Vol., L***	***[Tc], mol/L***	***Mass Tc, g***	***Percent Tc***
Feed (*A1*)	4.05	2.07×10^{-3}	8.29×10^{-1}	
Low acid scrub bottle 1 (*A5*)	0.85	1.37×10^{-3}	1.15×10^{-1}	13.9
Low acid scrub bottle 2 (*A5*)	0.67	7.54×10^{-4}	5.01×10^{-2}	6.0
Raffinate (*A4*)	4.76	(a)	6.33×10^{-2} (b)	7.6
Loaded solvent (*O2*)	11.00	5.51×10^{-4}	6.00×10^{-1}	72.4

(a) The Tc concentration in the aqueous raffinate solution could not be determined by ICP-MS because of its relatively low concentration coupled with isobaric interferences from other elements present in the solution (e.g., Ru).

(b) The mass of Tc in the raffinate was determined by subtracting the amount of Tc found in the two low acid scrub bottles and the loaded solvent from the amount of Tc in the feed solution.

(a) Using the mass of Tc estimated this way to be in the raffinate (6.33×10^{-2} g), and the volume of the raffinate (4.76 L), the Tc concentration in the raffinate was estimated to be 1.334×10^{-4} M.

Table 3.11. Technetium behavior during the Pu stripping step.

Process Stream	***Vol, L***	***[Tc], mol/L***	***Mass Tc, g***	***Percent Tc***(a)
Loaded solvent (*O2*)	10.62	5.51×10^{-4}	5.80×10^{-1}	
Product bottle 1 (*A8*)	0.87	3.48×10^{-4}	2.99×10^{-2}	5.1
Product bottle 2 (*A8*)	0.87	6.17×10^{-4}	5.31×10^{-2}	9.0
Product bottle 3 (*A8*)	0.89	6.21×10^{-4}	5.49×10^{-2}	9.3
Product bottle 4 (*A8*)	0.97	6.34×10^{-4}	6.09×10^{-2}	10.4
Product bottle 5 (*A8*)	0.97	6.16×10^{-4}	5.88×10^{-2}	10.0
Product bottle 6 (*A8*)	0.90	5.70×10^{-4}	5.06×10^{-2}	8.6
Product bottle 7 (*A8*)	0.91	5.99×10^{-4}	5.40×10^{-2}	9.2
Product bottle 8 (*A8*)	0.62	5.89×10^{-4}	3.63×10^{-2}	6.2
Pu-Depleted Solvent (*O4*)	14.67	1.30×10^{-4}	1.89×10^{-1}	32.1
Tc Recovered			5.87×10^{-1}	
Recovery, %			101%	

(a) Percentage based on the total Tc recovered in the product bottles and the Pu-depleted solvent.

3.3.2.5 Other Fuel Components

During solvent loading, 28% of the Zr reported to the aqueous raffinate, while 69% of the Zr was found in the low acid scrub outlet stream. The remaining 3% of the Zr was in the loaded solvent. These values should be viewed as indicative only since the Zr mass recovery was low (77%) for the solvent loading step. Zirconium was not detected in the U/Pu/Np product, so presumably it remained in the organic phase during the stripping portion of the test.

The behavior of Mo during solvent loading was difficult to assess because the analytical recovery of this element was very low (25%). Of the Mo detected in the process output streams, 93% was in the raffinate and 7% was in the loaded solvent. No Mo was detected in the U/Pu/Np product. Good recovery (102%) of Ru was obtained during the solvent loading step. The Ru was split between the raffinate (95.1%) and the loaded solvent (4.9%). No Ru was detected in the U/Pu/Np product. Like Mo, very low recovery (21%) of Pd was achieved during the solvent loading step; this was found completely in the raffinate solution.

As expected, the extraction of the lanthanide elements was low—less than 1% for La, Pr, Nd, and Eu. Samarium and Gd extracted to greater extents with 1.2% of the Sm and 4.1% of the Gd reporting to the loaded solvent. Recoveries for the lanthanide element during solvent loading were between 86 and 96%. Surprisingly, neither Sm or Gd were detected in the U/Pu/Np product, but these elements were detected in the Pu-depleted solvent. This result is unexpected given the low affinity of TBP for trivalent lanthanides.

3.3.2.6 Nitric Acid

Nitric acid was a target analyte to be determined by the on-line monitoring system, primarily through the Raman spectroscopic monitoring. To assess the effectiveness of the on-line monitoring system in determining HNO_3 concentration, the data obtained for the HNO_3 concentration in the U/Pu/Np product by the on-line monitor was compared to the data obtained by titration of selected grab samples and product bottle samples (Figure 3.1). The HNO_3 concentration values determined by the on-line monitor were consistently about 30% higher than those obtained by titration. Similar observations were made in previous CoDCon runs.[4] Further refinement of the chemometric model for HNO_3 determination is required to improve accuracy. Because work in the project was focus mainly on accurate determination of the U/Pu ratio, less effort was expended to optimize the model for HNO_3 determination. However, the pathway to improvement of this aspect of the model is well understood.

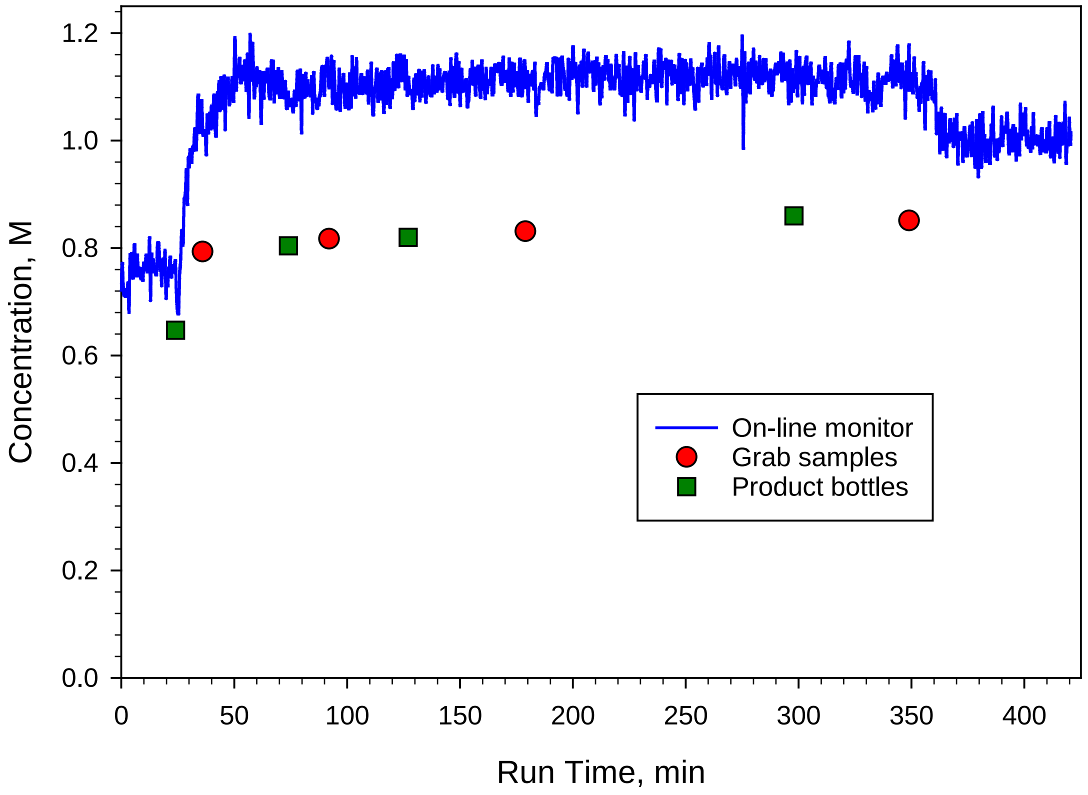

Figure 3.1. Nitric acid concentrations in the U/Pu/Np product stream determined by the on-line monitoring system and by titration of grab samples and samples taken from the product bottles.

3.3.3 Evolution of the Uranium-to-Plutonium Ratio During Run 5

Figure 3.2 presents the relative mass fractions of U and Pu in the aqueous product stream (*A8*) over the course of the experiment. There is generally good agreement between the on-line monitoring data and the off-line absorption spectroscopic analysis of the grab samples. However, absorptions spectroscopic analysis of the product bottles indicated the relative Pu content to be higher (when considering all U to be present in the +4 oxidation state, which was the case in previous CoDCon tests). The likely explanation for this is Tc-catalyzed decomposition of $N_2H_5NO_3$ in the product bottles, which would have caused more rapid oxidation of U(IV) to U(VI) in the product bottles than was observed in previous runs (in which Tc was not present). As indicated above, a substantial portion of the Tc (almost 50%) ended up in the U/Pu/Np product. Accurate quantification of U(VI) by absorption spectroscopy was vitiated by the presence of another unknown species with absorption in the same spectral region as U(VI). The results for the U/Pu ratio obtained by ICP-MS, both for grab samples, and the product bottles, agreed very well with the on-line monitoring result. This supports the conclusion that the off-line analysis of the product bottles by absorption spectroscopy was unreliable.

During the stripping step, various adjustments to the flow of the TBP solvent (*O3*) were made to achieve the target U/Pu ratio of 7/3. The adjustments made are summarized in Table 3.12, and these changes are represented by the vertical dashed lines in Figure 3.2. The average flowrate for the TBP solvent over the course of the stripping step was 10.6 ± 0.8 mL/min as determined by the change in the solvent vessel mass (Table 3.2), which is consistent with the values given in Table 3.12, which were determined from the flow meter calibration data. The adjustments made were effective at maintaining the target U/Pu ratio. It took 90 minutes to reach a relatively steady product stream, but from 90 minutes until the end of the test (over 400 min) the average relative U and Pu percentages were 69.3 ± 0.6 % and 30.7 ± 0.6 %, respectively. These averages are based on the on-line monitoring data over that time span. The average flowrate for the fresh TBP solvent during this stable period of operation was 10.8 ± 0.6 mL/min (determined by timed changes in the vessel mass) or 11.4 ± 0.5 mL/min (determined by flow meter).

Occasional transient drifts off the target U/Pu value were indicated by the on-line monitor over the course of the run. In one case, it was possible to obtain grab samples of the U/Pu product both during the drift and shortly thereafter (aqueous grab samples 4 and 5). Off-line spectroscopic analysis and ICP-MS analysis of these grab samples verified the transient drift in the U/Pu ratio (Figure 3.2). This indicated that the observed drift was not due to drifting in the on-line monitoring equipment, but rather was attributable to the intrinsic variability in the solvent extraction equipment performance.

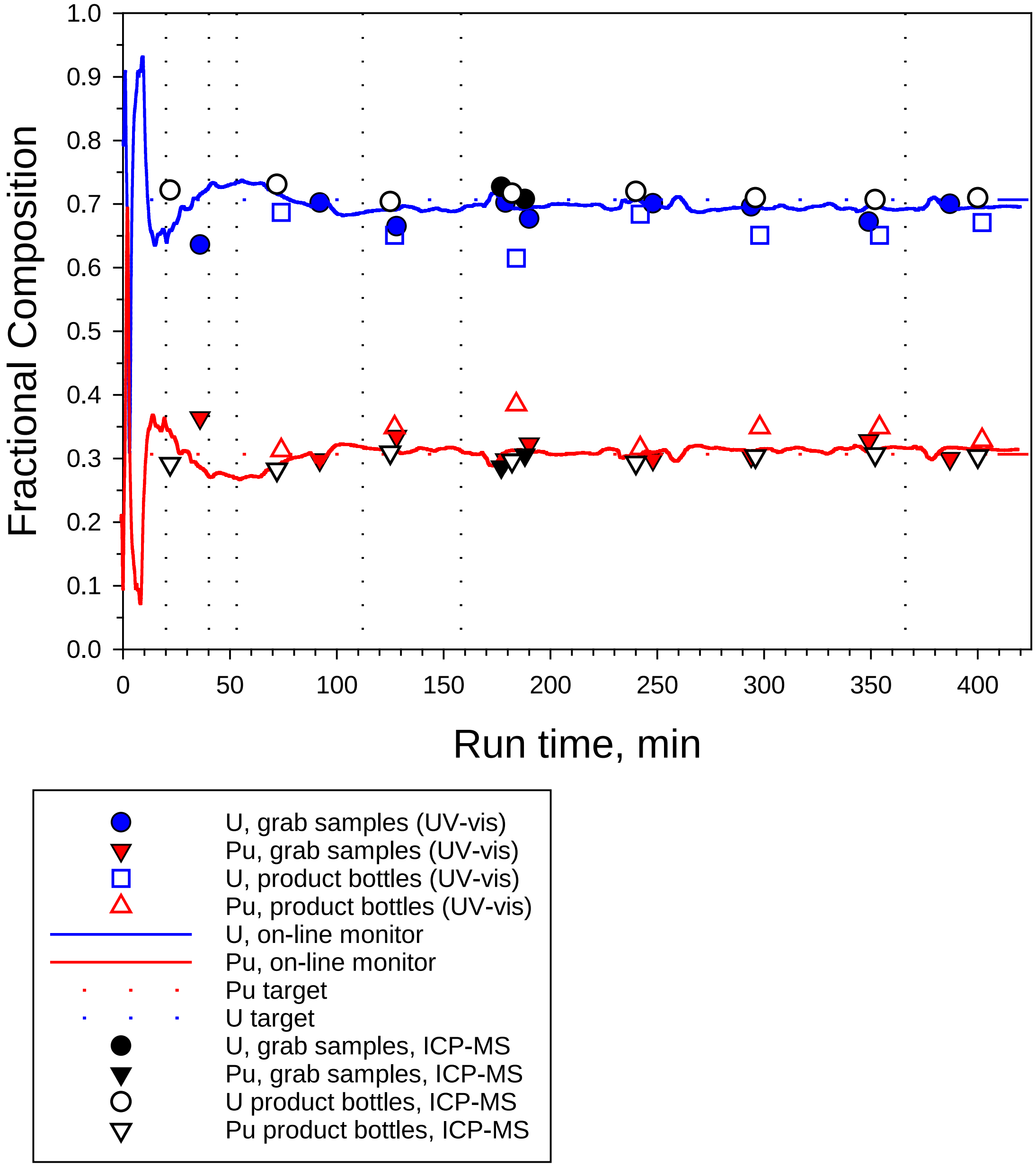

Figure 3.2. Uranium and Pu fractions in the aqueous product (*A8*) from CoDCon Run 5 as a function of run time (t = 0 at the point the loaded solvent was introduced into the stripping contactor bank). Data are presented from the on-line monitoring analysis, and separate spectroscopic and ICP-MS analyses of grab samples and the product bottles.

Figure 3.3 presents the U and Pu concentrations in the aqueous product stream (*A8*) over the course of the experiment as determined by the on-line monitoring system and by ICP-MS. The U and Pu concentrations determined by ICP-MS were typically lower than those determined by the on-line spectroscopy. This was especially true for product bottles 6 – 8. However, the uncertainty in the ICP-MS results is estimated to be 15%. If this uncertainty is applied (error bars in Figure 3.3), the U concentration values determined by ICP-MS fall within range of the on-line monitoring values, and the Pu values are generally in range, or close to within range. Because the relative U/Pu ratios agree very well between the two techniques (Figure 3.2), it is likely that the serial dilutions made to prepare samples for ICP-MS are mostly responsible for the differences between the two data sets.

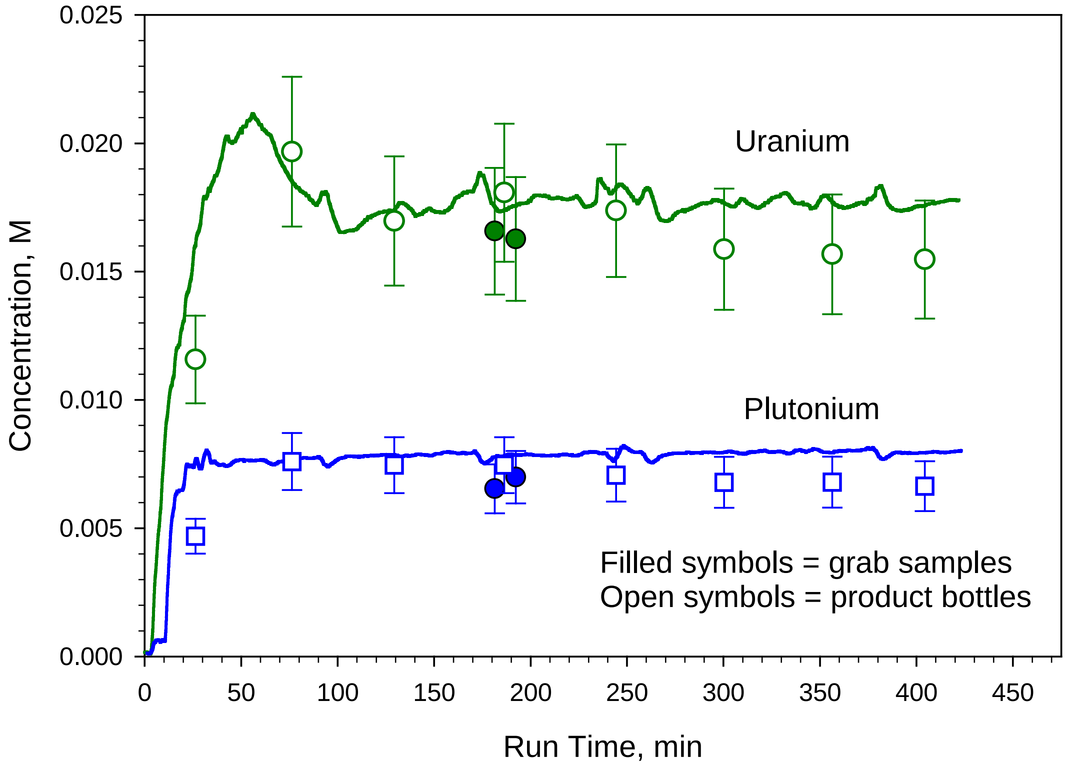

Figure 3.3. Uranium and Pu concentrations in the aqueous product stream (*A8*) during the stripping step, as determined by on-line monitoring (solid curves) and ICP-MS (symbols; circles = U, squares = Pu).

Table 3.12. Adjustments made to the TBP solvent (stream *O3*) flowrate during the CoDCon Run 5 stripping step.

Run time, min	TBP flowrate, mL/min[(a)]
0	9.4
22	8.9
42	9.4
55	10.9
114	10.7
160	10.4
368	10.2

(a) Flowrate based on pump calibration line.

3.4 AMUSE Modeling of the CoDCon Flowsheet

The AMUSE code was used to design the Run 5 CoDCon flowsheet using a simplified feed to speed the development process. For this design effort, the simplified feed included the key species for processing U, Pu, Np, and Tc. After performing the test, the flowsheet was again evaluated by AMUSE using model inputs that were based on the conditions actually encountered in the test. Like the Run 5 test itself, the AMUSE calculations were performed in two parts—the loading step and the Pu stripping step.

Table 3.13 compares the AMUSE result to the experimental result for the solvent loading step. The U concentration in the loaded solvent (*O2*) predicted by AMUSE agrees well with that measured experimentally. The measured U concentration in the raffinate (*A4*) was an orders-of-magnitude greater than predicted, but this still represented a very small percentage of the U (see also Table 3.4). The amount of U lost to the low acid scrub output stream (*A5*) agrees very well with the AMUSE prediction. Similar results were obtained for the behavior of Pu, with good agreement between the predicted and measured amounts of Pu in the loaded solvent stream and the low acid scrub stream. The measured value of Pu in the raffinate is two orders-of-magnitude greater than that predicted by AMUSE.

For the AMUSE calculation, the Np present in the feed was assumed to be 50% Np(V) and 50% Np(VI). The Np valence distribution is user-defined and is not adjusted during the simulation. As expected, the model indicated that any Np(V) present is directed completely to the raffinate. The results for Np in Table 3.13 are based on input of Np as Np(VI) in the AMUSE model. The predicted loss of Np to the raffinate stream is five orders-of-magnitude less than that observed. Also, the experimentally observed Np loss to the low acid scrub output stream is substantially greater than predicted by AMUSE. The high loss to the low acid scrub output is likely due to the presence of Np(V) during the flowsheet test, either through incomplete conversion to Np(VI) by the reaction with V(V) (equation 3.1), or by subsequent reduction of Np(VI) to Np(V). We hypothesize that the latter was the case, based on the following mechanism. First, contact with the low-acid scrub solution promotes disproportionation of Pu(IV) according to the following reaction.[12]

$$3Pu^{4+} + 2H_2O \rightleftharpoons 2Pu^{3+} + PuO_2^{2+} + 4H^+ \qquad (3.2)$$

Support for this comes from the off-line[(a)] vis-NIR absorption spectroscopic analysis of the low acid scrub collection bottles, which revealed the presence of Pu(VI) (see Appendix A). It should be noted that there was no spectroscopic evidence for Pu(VI) in the feed solution; the Pu was 100% Pu(IV) in the feed. So, disproportionation is assumed to have occurred in the low-acid scrub stages. Second, the Pu(III) formed through reaction 3.2 reduces Np(VI) to Np(V), and Np(V) is stripped from the solvent into the aqueous phase (that is, stream *A5*). This mechanism would account for the observed higher losses of Np to stream *A5* than predicted by AMUSE.

The AMUSE prediction for the Tc concentration in the loaded solvent agreed very well with that observed. However, the original modeling of the flowsheet suggested this would be about two orders-of-magnitude lower. The difference can likely be attributed, at least partially, to co-extraction of Tc with Zr (Zr was not included in the simple feed during development of the flowsheet *via* AMUSE). The AMUSE model predicts substantial extraction of Zr, which would be expected to result in co-extraction of TcO_4^-.[13] The low-acid scrub removes a significant fraction of the Zr from the solvent, but such conditions are not conducive to stripping of TcO_4^-, which can remain in the solvent associated with U and/or Pu.

Table 3.14 compares the AMUSE result to the experimental result for the Pu stripping step. The AMUSE result for the U/Pu/Np product (*A8*) disagrees with the experimental result. The U/(U+Pu) mass ratio predicted by AMUSE is only 0.094, whereas the measured value is 0.704.[(b)] Such a discrepancy was not observed when modeling earlier versions of the CoDCon flowsheet. As the U in the product is dominated by U(IV), the modeling of U(IV) in AMUSE should be re-examined. The U(IV) model was modified between CoDCon Runs 2 and 3, so these modifications may have adversely affected the predicted U(IV) behavior. Good agreement is seen in the predicted and experimental results for Np and Tc. Zirconium was mostly retained in the solvent phase during the Pu stripping portion of the flowsheet, which does not agree with what was predicted.

The distribution ratio of U(IV) between the aqueous nitrate solution and a solution of 30% TBP in dodecane, as well as the oxidation reactions U(IV) can undergo in the aqueous and organic phases was evaluated in a previous study.[14] The results of this analysis were incorporated into the AMUSE code. The U(IV) representation included addition of a hydrolyzed species to the aqueous phase, and the conjecture that one hydroxo group replaces one molecule of water, and that one nitrate group replaces two molecules of water in the hydration shell. The following equation for the distribution coefficient the following equation was utilized for modeling the distribution coefficient for U(IV) where *n* is the hydration number. Figure 3.4 shows the experimental and the calculated distribution coefficients using equation (3.3) for different values of K and hydration numbers.

$$D_{U(IV)} = \frac{K\{NO_3\}^4\{TBP_f\}^2}{(1+\beta_{1-NO_3}\frac{\{NO_3\}}{\{H_2O\}^2}+\beta_{2-NO_3}\frac{\{NO_3\}^2}{\{H_2O\}^4}+K_{H1}\frac{1}{\{H^+\}\{H_2O\}})\cdot\{H_2O\}^n} \tag{3.3}$$

[(a)] The low-acid scrub output stream was not monitored using the on-line monitoring system during the experiment. Rather, samples were taken for off-line analysis.

[(b)] The AMUSE predicted U concentration is $5.08 \times 10^{-6} + 6.97 \times 10^{-4} = 7.02 \times 10^{-4}$ M or 0.167 g U/L. The AMUSE predicted Pu concentration is 6.71×10^{-3} M or 1.60 g Pu/L. Giving a U/Pu mass ratio of 0.167/(0.167 + 1.60) = 0.094. The corresponding measured values are for U, 1.64×10^{-2} M or 3.90 g U/L, and for Pu, 6.86×10^{-3} M or 1.64 g Pu/L; giving a U/Pu ratio of 3.90/(3.90 + 1.64) = 0.704.

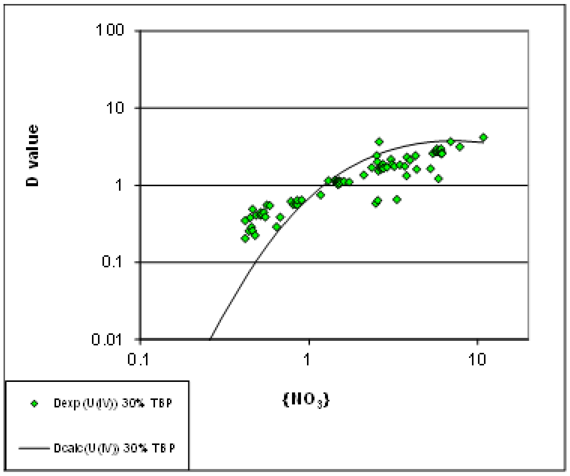

Figure 3.4. Experimental and calculated distribution coefficients for U(IV) between 30% TBP in dodecane and aqueous nitrate solution; with hydration number = 9 and K = 4.8 in eqn. Taken from reference [14].

As can be seen from Figure 3.4, the U(IV) model tends to over-predict the D-value for acid concentrations above one molar, while it under-predicts values below 0.8 M. Because this transition occurs in the region where the test second segment operates, small variations in H^+ loading of the incoming loaded solvent had a strong effect on the U(IV) extraction profiles. The U(IV) D-value was below 1.0 for all stages in the scrub and the U/Pu strip sections.

Table 3.13. Comparison of concentrations for selected components calculated by AMUSE to the measured values for the solvent loading section of the Run 5 CoDCon flowsheet.

Stream	Flow, mL/min	Uranium		Plutonium		Neptunium		Technetium		Zirconium	
		Calcd.	Found	Calcd.	Found	Calcd.	Found	Calcd.	Found	Calcd.	Found
O1	31.7(a)	NA	NA	NA	NA	NA	NA	NA	NA	NA	NA
A1	10.9(a)	1.10×10^{0} (a)	1.10×10^{0}	1.46×10^{-2} (a)	1.46×10^{-2}	6.10×10^{-4} (a,b)	1.22×10^{-3} (c)	2.07×10^{-3} (a)	2.07×10^{-3}	1.90×10^{-2} (a)	9.93×10^{-3}
A2	3.3(a)	NA	NA	NA	NA	NA	NA	NA	NA	NA	NA
A3	5.0(a)	NA	NA	NA	NA	NA	NA	NA	NA	NA	NA
A4	14.2	1.08×10^{-6}	1.89×10^{-5}	1.80×10^{-8}	1.22×10^{-6}	3.49×10^{-10}	1.19×10^{-5}	2.41×10^{-6}	(d)	2.78×10^{-4}	1.82×10^{-3}
A5	5.0	1.56×10^{-1}	1.62×10^{-1}	5.58×10^{-3}	6.45×10^{-3}	2.26×10^{-5}	1.13×10^{-3}	2.74×10^{-4}	1.06×10^{-3}	3.79×10^{-2}	1.42×10^{-2}
O2	31.7	3.53×10^{-1}	3.51×10^{-1}	4.11×10^{-3}	4.09×10^{-3}	2.06×10^{-4}	2.39×10^{-4}	6.66×10^{-4}	5.51×10^{-4}	2.41×10^{-4}	9.26×10^{-5}

(a) Input into AMUSE.

(b) Entered as Np(VI) in the feed solution for the AMUSE calculation.

(c) Measured as total Np.

(d) Could not be accurately measured, but estimated to be 1.3×10^{-2} M from the estimated mass of Tc in Table 3.10, and the total volume of the raffinate (4.76L).

NA = Not Applicable

Table 3.14. Comparison of concentrations for selected components calculated by AMUSE to the measured values for the Pu stripping section of the Run 5 CoDCon flowsheet.

Stream	Flow, mL/min	Uranium		Plutonium		Neptunium		Technetium		Zirconium	
		Calcd.	Found	Calcd.	Found	Calcd.	Found	Calcd.	Found	Calcd.	Found
O3	11.3(a)	NA	NA	NA	NA	NA	NA	NA	NA	NA	NA
O2	27.9(a)	3.58×10^{-1} (a,b)	3.51×10^{-1}	4.33×10^{-3} (a,c)	4.09×10^{-3}	1.04×10^{-4} (d)	2.39×10^{-4}	6.72×10^{-4} (a)	5.51×10^{-4}	3.00×10^{-4} (a)	9.26×10^{-5}
A6	2.6(a)	NA	NA	NA	NA	NA	NA	NA	NA	NA	NA
A7	15.4(a)	8.12×10^{-3} 4.01×10^{-2} (e)	5.29×10^{-2}	NA	NA	NA	NA	NA	NA	NA	NA
A8	18.0	5.08×10^{-6} 6.97×10^{-4} (e)	1.64×10^{-2}	6.71×10^{-3}	6.86×10^{-3}	1.61×10^{-4}	3.72×10^{-4}	1.74×10^{-4}	6.05×10^{-4}	4.65×10^{-4}	Not detected
O4	39.2	2.58×10^{-1} 1.54×10^{-2} (e)	2.56×10^{-1}	1.23×10^{-9}	Not detected	2.87×10^{-11}	Not detected	3.98×10^{-4}	1.30×10^{-4}	1.33×10^{-10}	1.49×10^{-4}

(a) Input into AMUSE.

(b) As U(VI).

(c) Input as Pu(III).

(d) Input as Np(V).

(e) Upper value is U(VI), lower value is U(IV).

NA = Not Applicable

4.0 Conclusions

Five CoDCon flowsheet tests were conducted. In all five cases, on-line optical spectroscopy, coupled with chemometric modeling of the spectral data, provided real-time information regarding the U/Pu ratio in the product stream. This real-time process solution information was used to manipulate the process conditions to achieve the targeted U/Pu mass ratio of 7/3. Although this methodology proved effective, the stability of the solvent extraction system was not always consistent from run to run. Very stable operation of the system was achieved during CoDCon Runs 2, 3, and 5; but much more drift in the system was experienced in Runs 1 and 4.

Table 4.1 provides a comparison of the results from the five CoDCon flowsheet tests in terms of the U and Pu fractions in the product bottles. For Runs 2,[4] 3,[5] and 5 the data presented in Table 4.1 represent the average composition of the product bottles taken during the most stable period of operation (representing three product bottles for Run 2, seven product bottles for Run 3, and six product bottles for Run 5). As can be seen, during these stable periods of operation the standard deviation in the percent composition was very low (< 1%). On the other hand, stable periods of operation were more elusive in Runs 1[4] and 4.[5] In these cases, the standard deviations in the composition of product was ~3%. Based on the limited set of data represented by these five CoDCon tests, it is reasonable to conclude that the U/Pu ratio can easily be maintained within 5% of a target ratio using the laboratory-scale solvent extraction system used in this work.(a) Application of online optical spectroscopic monitoring is an essential tool for controlling the target U/Pu ratio.

Table 4.1. Comparison of the U and Pu fractions in the product bottles from the four CoDCon flowsheet tests.

Run #	***U, %***	***Pu, %***	***Standard Deviation, %***
1	61.4	38.6	2.8
2	70.4	29.6	0.1
3	70.3	29.7	0.4
4	69.7	30.3	2.5
5	70.4	29.6	0.6

(a) The reason for the low relative U content of the product from Run 1 has previously been discussed.[1] It was attributed to a false indication of U(VI) in the U/Pu nitrate product stream by the chemometric model. This issue was subsequently corrected.

5.0 Publications

The following is a list of publications that resulted from the CoDCon project.

1. Sinkov S.I., G.B. Hall, and G.J. Lumetta. 2020. Molar Absorptivities of U(VI), U(IV), and Pu(III) in Nitric Acid Solutions of Various Concentrations Relevant to Developing Nuclear Fuel Recycling Flowsheets, *Journal of Radioanalytical and Nuclear Chemistry* 324, no. 2:773-789
2. Lines A.M., G.B. Hall, S.E. Asmussen, J.R. Allred, S.I. Sinkov, F.D. Heller, and N.B. Gallagher, et al. 2020. Sensor fusion: comprehensive real-time, on-line monitoring for process control via visible, NIR, and Raman spectroscopy, *ACS Sensors*. Ahead of Print: https://doi.org/10.1021/acssensors.0c00659
3. Lines A.M., G.B. Hall, S.I. Sinkov, T.G. Levitskaia, N.B. Gallagher, G.J. Lumetta, and S.A. Bryan. 2020. Overcoming oxidation state dependent spectral interferences: On-line monitoring of U(VI) reduction to U(IV) via Raman and UV-vis spectroscopy, *Industrial and Engineering Chemistry Research* 59, no. 19:8894-8901
4. Lumetta G.J., F.D. Heller, G.B. Hall, S.E. Asmussen, and S.I. Sinkov. 2020. Optical Spectroscopic Investigation of Hexavalent Actinide Ions in n-Dodecane Solutions of Tri-butyl Phosphate, *Solvent Extraction and Ion Exchange*. Ahead of Print: https://doi.org/10.1080/07366299.2020.1805051
5. Lumetta, G.J., J.R. Allred, S.A. Bryan, G.B. Hall, T.G. Levitskaia, A.M. Lines, S.I. Sinkov. 2019. Simulant testing of a co-decontamination (CoDCon) flowsheet for a product with a controlled uranium-to-plutonium ratio, *Separation Science and Technology*, 54 no. 12, 1977-1984
6. Lines, A.M., S.R. Adami, S.I. Sinkov, G.J. Lumetta, S.A. Bryan. 2017. Multivariate Analysis for Quantification of Plutonium (IV) in Nitric Acid Based on Absorption Spectra, *Analytical Chemistry* 89 no. 17:9354-9359
7. Lines, A.M., S.R. Adami, A.J. Casella, S.I. Sinkov, G.J. Lumetta, S.A. Bryan. 2017. Electrochemistry of the Pu (III/IV) and (IV/VI) Couples in Nitric Acid Systems, *Electroanalysis 29 no 12:2744-2751*
8. G.J. Lumetta, J.R. Allred, S.E. Asmussen, S.A. Bryan, G.B. Hall, F.D. Heller, A.M. Lines, and S.I. Sinkov, “Progress in Real-time Monitoring for Controlling the Composition of the Uranium-Plutonium Nitrate Product in a Tri-butyl Phosphate Based Flowsheet,” *Global 2019*, Seattle, Washington, September 22 – 27, 2019; American Nuclear Society, La Grange Park, Illinois; pp. 993-998
9. A.M. Lines, S.D. Branch, H.M. Felmy, J.M. Wilson, G.J. Lumetta, and S.A. Bryan, “On-Line Monitoring Combined with Spectroelectrochemistry for the Characterization of Uranium and Fission Products Within Molten Salt Environments,” *Global 2019*, Seattle, Washington, September 22 – 27, 2019; American Nuclear Society, La Grange Park, Illinois; pp. 1104-1106
10. J., Bresee, P. Paviet, D. Vega, G. Lumetta, M. Miller, and T. Todd, “The Alliance of Advanced Process Control and Accountability – A Future Safeguards-By-Design Tool,” 58th INMM Annual Meeting, July 16 – 20, 2017, Indian Wells, California; Institute of Nuclear Materials Management, Oakbrook Terrace, Illinois.

6.0 References

1. Lumetta, G. J.; Casella, A. J.; Sevigny, G. J.; Bryan, S. A.; Hall, G. B.; Levitskaia, T. G.; Lines, A. M.; Allred, J. R.; Orton, R. D. *CoDCon Project: Design of the Phase 1 Testing System*; PNNL-26173 (FCRD-MRWFD-2017-000359); Pacific Northwest National Laboratory: Richland, Washington, 2017.
2. Bresee, J.; Paviet, P.; Vega, D.; Lumetta, G.; Miller, M.; Todd, T. The Alliance of Advanced Process Control and Accountability – A Future Safeguards-By-Design Tool. In *58th Institute of Nuclear Materials Management Annual Meeting*, Institute of Nuclear Materials Management: Indian Wells, California, 2017.
3. Lines, A. M.; Hall, G. B.; Asmussen, S.; Allred, J.; Sinkov, S.; Heller, F.; Gallagher, N.; Lumetta, G. J.; Bryan, S. A. Sensor Fusion: Comprehensive Real-Time, On-Line Monitoring for Process Control via Visible, Near-Infrared, and Raman Spectroscopy. ACS Sensors **2020,** *5*, 2467-2475.
4. Lumetta, G. J.; Allred, J. R.; Bryan, S. A.; Hall, G. B.; Heller, F. D.; Levitskaia, T. G.; Lines, A. M.; Sinkov, S. I. *CoDCon Project: FY 2018 Status Report*; PNNL-27850 (NTRD-MRWFD-2018-000224); Pacific Northwest National Laboratory: Richland, Washington, 2018.
5. Lumetta, G. J.; Allred, J. R.; Asmussen, S. E.; Bryan, S. A.; Carter, J. C.; Hall, G. B.; Heller, F. D.; Lines, A. M.; Sinkov, S. I. *CoDCon Project: FY 2019 Status Report*; PNNL-28983; Pacific Northwest National Laboratory: Richland, Washington, 2019.
6. Dukes, E. K. *Oxidation of Neptunium(V) by Vanadium(V)*; DP-434; E. I. du Pont de Nemours & Co. Savannah River Laboratory: Aiken, SC, 1959.
7. Koch, G. *Recovery of By-Product Actinides from Power Reactor Fuels*; KFK-976; Kernforschungszentrum Karlsruhe: Karlsruhe, Germany, 1969.
8. Leonard, R. A.; Bernstein, G. J.; Ziegler, A. A.; Pelto, R. H. Annular Centrifugal Contactors for Solvent Extraction. Sep. Sci. Technol. **1980,** *15*, 925-943.
9. Sakurai, S.; Miyauchi, M.; Tachimori, S. Density Equations of $UO_2(NO_3)_2$-HNO_3 and $UO_2(NO_3)_2$-$Gd(NO_3)_3$-HNO_3 Solutions. J. Nucl. Sci. Technol. **1987,** *24* (5), 415-419.
10. Ryan, J. L.; Bryan, G. H.; Burt, M. C.; Costanzo, D. Preparation of Standards for and Determination of Free Acid in Concentrated Plutonium–Uranium Solutions. Anal. Chem. **1985,** *57*, 1423-1427.
11. Precek, M. The Kinetic and Radiolytic Aspects of Control of the Redox Speciation of Neptunium in Solutions of Nitric Acid. Oregon State University, Corvallis, Oregon, 2012.
12. Cleveland, J. M. *The Chemistry of Plutonium*. Gordon and Breach Science Publishers: New York, 1970.
13. Herbst, R. S.; Baron, P.; Nilsson, M. Standard and advanced separation: PUREX processes for nuclear fuel reprocessing. In *Advanced Separation Techniques for Nuclear Fuel Reprocessing and Radioactive Waste Treatment*; Nash, K. L.; Lumetta, G. J., Eds; Woodhead Publishing: Oxford, 2011; pp 141-175.
14. Lichtenberger, J.; Copple, J.; Pereira, C. *CoDCon Flowsheet Chemistry and Design*; ANL/20-69; Argonne National Laboratory: Lemont, Illinois, 2018.

Appendix A

Off-line Spectrophotometric Analysis Results of Low Acid Scrub samples in Run 5

Eight grab samples and two collection bottles of the low acid scrub effluent (stream *A5*) were collected during the loading step of Run 5. These samples were measured with two instruments—first covering the spectral range from 350 to 950 nm (Spectral Instruments, model 420), and then, with minimal time delay, scanning the spectral range 900-1100 nm (Ocean Optics USB 2000). The second scanning was performed to detect the potential presence of Np(V) using its strong and well-defined absorbance peak at 981.64 nm. Figure A1 shows spectra of eight low acid scrub samples measured 1 to 2 hours after collection.

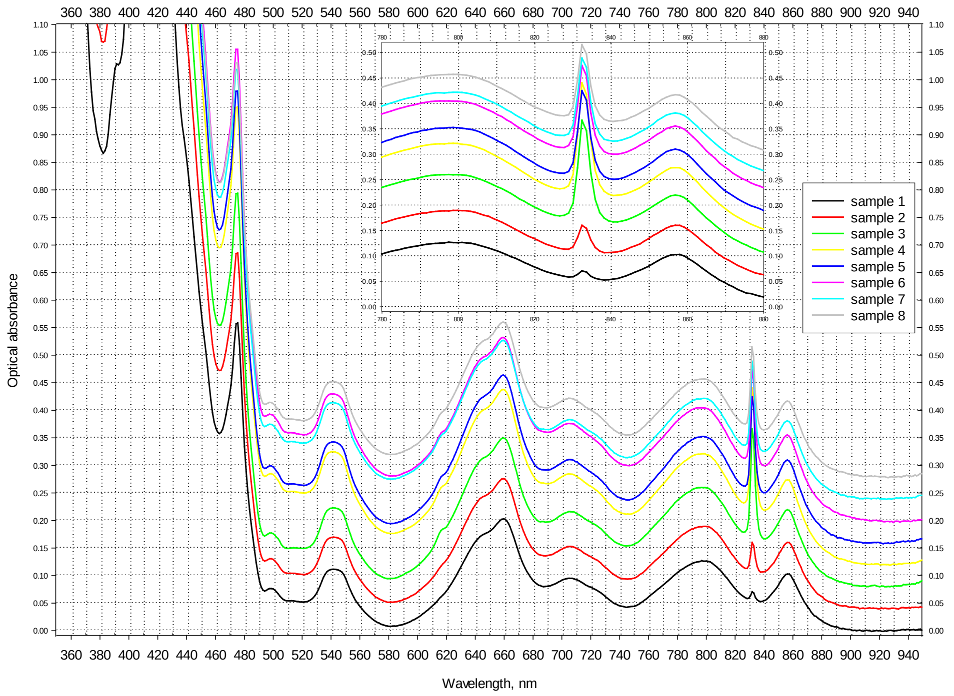

All scrub samples, rezeroed at 920 nm and offset by 0.00, 0.04, 0.08, 0.12, 0.16, 0.20, 0.24, and 0.28 absorbance units for s01, s02, ..., s08 respectively.

Figure A1. Optical absorbance spectra of low acid scrub grab samples collected in 350-950 nm spectral range. Spectra of samples s01 to s08 are re-zeroed at 920 nm and then offset for clarity by 0.04 absorbance for each next spectrum starting from s02.

It is seen that the spectra presented have significant contribution not only from Pu(IV) (peaks at 476, 542, 660, 708, 798 and 872 nm, but, more surprisingly, from Pu(VI) (sharp peak at 832.48 nm). It is noteworthy that all Pu in the aqueous feed for Run 5 was represented exclusively by Pu(IV) with no spectral evidence for Pu(VI). The most likely explanation of appearance of Pu(VI) in the low acid scrub stream is the partial disproportionation reaction of Pu(IV) to lower [Pu(III)] and higher [Pu(VI)] oxidation states of this element which can be expressed by the following equation:

$$3Pu^{4+} + 2H_2O \rightleftharpoons 2Pu^{3+} + PuO_2^{2+} + 4H^+ \tag{A1}$$

This disproportionation is favored by low acid conditions which indeed occurred when low acid scrub solution [10 mM V(V) in 0.05M HNO_3] entered the battery of contactors in the U(VI) and Pu(IV) loading process.

However, if reaction A1 does occur, it should generate 2 equivalents of Pu(III) per one equivalent of Pu(VI). In this process Pu(III) should be visible in the spectra presented as double peak feature at 562 and 601 nm and additional relatively sharp peak at 665 nm, which is not the case. Careful examination of the spectra (s02 to s08) in Figure A1 reveals a very small shoulder at 617 nm which might be an indication of pentavalent neptunium presence in this stream. To verify this possibility, additional spectral scans were performed in the near infra-red region. The results are shown in Figure A2.

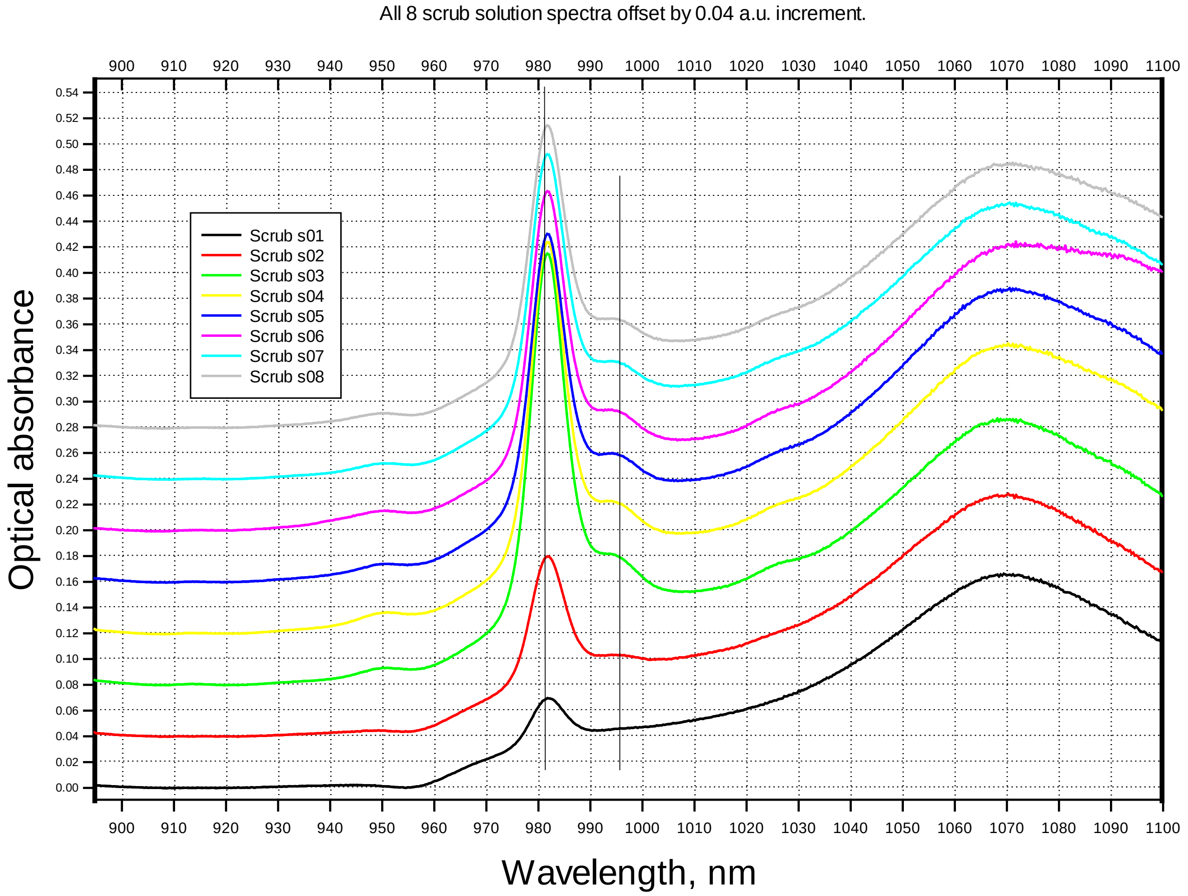

Figure A2. Optical absorbance spectra of low acid scrub grab samples collected in 900-1100 nm spectral range. Similar to figure A1, spectra of samples s01 to s08 are re-zeroed at 920 nm and then positively offset for clarity by 0.04 absorbance for each next spectrum starting from s02.

Spectra shown in Figure A2 exhibit a shoulder at ~ 996 nm, in addition to major peak of Np(V) at 981.64 nm and broad peak of Pu (IV) at 1070 nm. The former feature is an indication of complex formation between Np(V) and U(VI).[A1] According to ICP-MS data, the low acid scrub solutions contain U(VI) in concentrations ranging from 0.17 to 0.22 M, which is high enough to bind some fraction of Np(V) into the cation-cation complex under these conditions.

Comparison of Figures A1 and A2, not only clearly reveals simultaneous presence of two dioxocations of Pu(VI) and Np(V) in unexpectedly high concentrations with respect to aqueous feed, but qualitatively it appears that the magnitudes of these peaks are in good correspondence between each other for each particular sample (lower peak intensities for samples 1 and 2 are followed by progressively higher values for the next two samples (s03 and s04) after which the magnitudes go back to slightly lower values for the remaining 4 grab samples.

To see this correlation more clearly, net peak intensities of Np(V) are plotted versus peak intensities of Pu(VI) as shown in Figure A3.

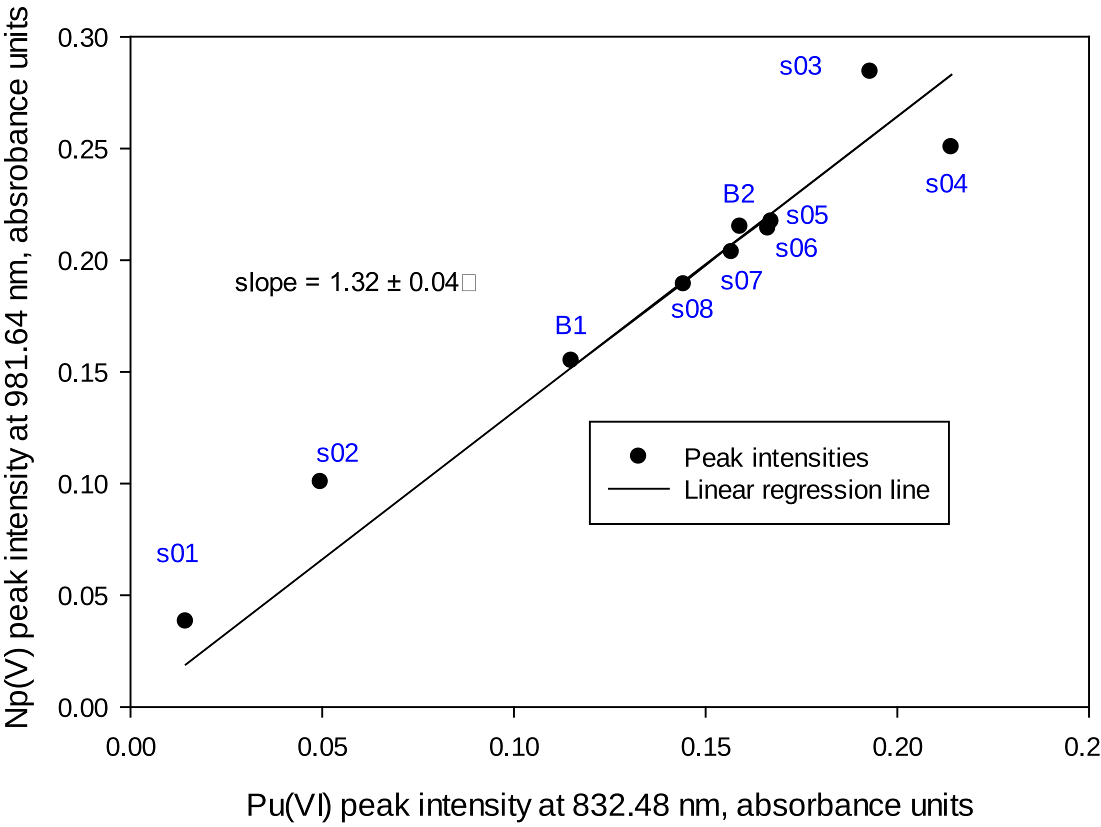

Figure A3. Relationship between peak intensities of Np(V) and Pu(VI) in the Low Acid Scrub samples (s01 to S08) and Low Acid Scrub Effluent bottles (points B1 and B2). Linear regression model applied for data processing is a straight line with zero intercept.

The absence of the Pu(III) signature in the spectral plots shown above is most likely associated with its interaction with hexavalent Np and full consumption of the former in this process according to the following reaction:[A2]

$$NpO_2^{2+} + Pu^{3+} = NpO_2^{+} + Pu^{4+} \qquad (A2)$$

So, considering equations (A1) and A(2) together, one can easily deduce that for each equivalent of Pu(VI) formed by the disproportionation reaction there should be two equivalents of Np(V) produced in which case all initially available Pu(III) reacts with Np(VI) to form Pu(IV). To check the validity of this hypothesis, peak intensities of Pu(VI) and Np(V) have to be converted to their concentrations to see at what concentration ratio these species are present in scrub solutions. Molar absorptivities of Np(V) and Pu(VI) were measured in our laboratory several years ago when work was performed on speciation of these oxidation states in HNO_3 solutions and values found are 350.8 M^{-1} cm^{-1} and 335.3 $M^{-1}cm^{-1}$ for Np(V) in 2M HNO_3 and 3M HNO_3 respectively, and 465 M^{-1} cm^{-1} for Pu(VI) in 1M HNO_3. The Np(V) value for 2.3 M HNO_3 acidity found in scrub solutions can be calculated by linear interpolation as 345.2 M^{-1} cm^{-1}. There is not enough data for Pu(VI) at higher acidity to do the same interpolation, but according to the literature molar absorptivity of Pu(VI) shows very little changes between 0 M HNO_3 ($HClO_4$ medium) and 3.4 M HNO_3,[A3] so the value of 465 $M^{-1}cm^{-1}$ can be used without a serious bias in this exercise.

Before the slope of regression line shown in Figure A3 can be converted to the Np(V) to Pu(VI) concentration ratio, one more correction regarding Np(V) concentration must be made. In the presence of ~0.2 M U(VI), the total Np(V) concentration is the sum of uncomplexed Np(V) and the portion of Np(V) bound into cation-cation complex with U(VI). It is known that binding constant of Np(V) complex formation with U(VI) is a sensitive function of ionic strength and most determinations were done at I = 6 M and higher. Fortunately, one study examined this process at I = 3 M [1] ($K_{Np5\cdot U6}$ = 0.69) which is close enough to our condition of 2.3 M HNO_3 + 0.2 M uranyl nitrate in terms of ionic strength.[A1] Application of this value gives [Np5·U6]/[Np5] ratio equal to 0.69*0.2 = 0.138, which means that free Np(V) concentration determined *via* peak intensity at 981.64 nm has to be multiplied by a factor of 1 + 0.138 = 1.138 to account for total Np(V) concentration. So the slope of regression line has to be multiplied by ratio of 465 to 345.2 and then scaled up by a factor of 1.138 to derive an average ratio of the total Np(V) to Pu(VI) concentrations in a series of low acid scrub samples. The result of this calculation is (1.32 ± 0.04) *465/345.2 *1.138 = 2.02 ± 0.06. The value calculated is in a very good correspondence with proposed mechanism of this process based on equations (A1) and (A2).

References

1. Sullivan, J.C., Hindman, J.C., Zielen, A.J. Specific Interaction between Np(V) and U(VI) in Aqueous Perchloric Acid Media. *J. Am. Chem. Soc.* 1961, 83, 3373-3378.
2. Fulton, R.B; Newton, T.W. The kinetics of the Oxidation of Plutonium(III) by Neptunium(VI). *The Journal of Physical Chemistry*, 1970, 74, 3, 1661-1669.
3. Gaunt, A.J., May, I., Neu, M.P., Reilly, S.D., Scott, B.L. Structural and Spectroscopic Characterization of Plutonyl(VI) Nitrate under Acidic Conditions. *Inorg. Chem.* 2011, 50, 4244-4246.